F1000Research

CrossMark
click for updates

RESEARCH ARTICLE

UPDATED I. Embryonal vasculature formation recapitulated in transgenic mammary tumor spheroids implanted pseudo-orthotopicly into mouse dorsal skin fold: the organoblasts concept [v2; ref status: indexed, http://f1000r.es/1fa]

Halina Witkiewicz, Phil Oh, Jan E Schnitzer

Proteogenomics Research Institute for Systems Medicine, San Diego, CA, 92121, USA

Abstract

Inadequate understanding of cancer biology is a problem. This work focused on cellular mechanisms of tumor vascularization. According to earlier studies, the tumor vasculature derives from host endothelial cells (angiogenesis) or their precursors of bone marrow origin circulating in the blood (neo-vasculogenesis) unlike in embryos. In this study, we observed the neo-vasculature form in multiple ways from local precursor cells. Recapitulation of primitive as well as advanced embryonal stages of vasculature formation followed co-implantation of avascular (*in vitro* cultured) N202 breast tumor spheroids and homologous tissue grafts into mouse dorsal skin chambers. Ultrastructural and immunocytochemical analysis of tissue sections exposed the interactions between the tumor and the graft tissue stem cells. It revealed details of vasculature morphogenesis not seen before in either tumors or embryos. A gradual increase in complexity of the vascular morphogenesis at the tumor site reflected a range of steps in ontogenic evolution of the differentiating cells. Malignant- and surgical injury repair-related tissue growth prompted local cells to initiate extramedullar erythropoiesis and vascular patterning. The new findings included: interdependence between the extramedullar hematopoiesis and assembly of new vessels (both from the locally differentiating precursors); nucleo-cytoplasmic conversion (karyolysis) as the mechanism of erythroblast enucleation; the role of megakaryocytes and platelets in vascular pattern formation before emergence of endothelial cells; lineage relationships between hematopoietic and endothelial cells; the role of extracellular calmyrin in tissue morphogenesis; and calmyrite, a new ultrastructural entity associated with anaerobic energy metabolism. The central role of the extramedullar erythropoiesis in the formation of new vasculature (blood and vessels) emerged here as part of the tissue building process including the lymphatic system and nerves, and suggests a cellular mechanism for instigating variable properties of endothelial surfaces in different organs. Those findings are consistent with the organoblasts concept, previously discussed in a study on childhood tumors, and have implications for tissue definition.

Article Status Summary

Referee Responses

Referees	1	2	3
v1 published 10 Jan 2013	❌ report 1	❓ report 1	✅ report 1
v2 published 11 Jul 2013 UPDATED	❌ report	✅ report	✅

1 **Louise Purton**, St Vincent's Institute Australia

2 **Anita Bandrowski**, University of California, San Diego USA

3 **Karolina Kucharova**, Sanford-Burnham Medical Research Institute USA

Latest Comments

No Comments Yet

Associated Research Article

Witkiewicz H, Oh P and Schnitzer JE » II. Capsular vaso-mimicry formed by transgenic mammary tumor spheroids implanted ectopically into mouse dorsal skin fold: implications for cellular mechanisms of metastasis, *F1000Research* 2013, **2**:9 (doi: 10.12688/f1000research.2-9.v2)

Witkiewicz H, Oh P and Schnitzer JE » III. Cellular ultrastructures in situ as key to understanding tumor energy metabolism: biological significance of the Warburg effect, *F1000Research* 2013, **2**:10 (doi: 10.12688/f1000research.2-10.v1)

Corresponding author: Halina Witkiewicz (hwitkiewicz@UCSD.edu)

How to cite this article: Witkiewicz H, Oh P and Schnitzer JE (2013) **I. Embryonal vasculature formation recapitulated in transgenic mammary tumor spheroids implanted pseudo-orthotopicly into mouse dorsal skin fold: the organoblasts concept [v2; ref status: indexed, http://f1000r.es/1fa]** *F1000Research* 2013, **2**:8 (doi: 10.12688/f1000research.2-8.v2)

Competing interests: No relevant competing interests were disclosed.

First published: 10 Jan 2013, **2**:8 (doi: 10.12688/f1000research.2-8.v1)
First indexed: 22 Jul 2013, **2**:8 (doi: 10.12688/f1000research.2-8.v2)

UPDATED **Changes from Version 1**

The 'Viewing' section of the Methods has been modified to provide further details on the process of selecting images to be captured.

The reason for including shorter incubation time has been clarified in the 'Experimental design' section of Material and Methods.

The two sentences singled out by the referee have been modified as follows: 1. (Introduction) 'However, the views on tumor neo-angiogenesis remained polarized[3,12]'. 2. (Results) 'A composite dense body resembling those seen in platelets[56] was found in one of the cells depositing elements of ECM (Figure 1 [E & F]) suggesting that the cell building ECM was related to the platelets producing cell type, i.e., to megakaryocyte'.

The acronyms have been listed in Materials and Methods.

The scale bar unit in Figure 10 [A] & Figure S10 [A] has been corrected.

Other comments made by the referees have been addressed in the referee reports section.

See referee reports

"The significant problems we face cannot be solved at the same level of thinking we were at when we created them".

– Albert Einstein

Introduction
Some of the unsolved problems in vascular biology

Tumor vascular biology research has been beleaguered with multiple controversial experimental data and unanswered questions despite the technological progress and new concepts in network biology. The importance of understanding interactions among individual elements of a system has only recently gained popularity. Much of the information on mapping of mammalian interactome networks waits to be experimentally validated, although advancements have been made in small model organisms (yeast, *Saccharomyces cerevisiae*; fruit fly, *Drosphila melanogaster*; and worm, *Caenorhabditis elegans*)[1]. Richness and redundancy enabling the natural selection of evolving biological systems make their analysis difficult and call for new methods and ways of thinking[2,3]. Unsolved problems include lineage relationship between endothelial stem cells (SCs) and hematopoietic stem cells (HSCs)[4,5]; the role of platelets in embryonal development[6,7]; lineages of immune cells[8], tolerance of tumors by the host immune system[9] and reprogramming of energy metabolism by tumors[5,9]. The question of biological significance of the cellular heterogeneity within tumors also remains unanswered.

Vasculogenesis versus angiogenesis

Traditionally vasculogenesis and hematopoiesis were subjects of independent studies and some fundamental issues have remained unclear in each case. The origin of the precursors of endothelial cells (ECs) has created controversy in understanding tumor growth related vasculogenesis, whereas the illusive origin of HSCs had been a daunting problem in understanding embryonal development. As opposed to *de novo* vasculature formation during embryogenesis (vasculogenesis), tumor vasculature has been thought to emerge by expansion of the host vasculature through postnatal sprouting of endothelial cells (angiogenesis). Therefore, it was proposed that inhibiting angiogenesis would stop tumor growth[10]. When that

conceptually simple objective turned out to be impossible to reach, a notion of neo-vasculogenesis was born, suggesting that tumor vessels form from circulating bone marrow-derived endothelial precursors rather than from mature ECs[11]. However, the views on tumor neo-angiogenesis remained polarized[3,12].

Erythropoiesis

Descriptions of the two main types of erythropoiesis, i.e. primitive and definitive, has kept changing over the years. Extremely large nucleated cells and smaller enucleated ones, distinguished first, were later referred to as nucleated and anuclear, respectively[13,14]. Each wave of erythropoiesis was reported to generate more potent progenitors (progenitors of more numerous cell types)[15]. Lately, five distinct classes of hematopoietic cells in murine conceptus emerged from studies on their activity in transplantation or clonogenic assays *in vitro*: primitive; pro-definitive (myeloid progenitors); meso-definitive (lymphoid-myeloid progenitors); meta-definitive (neonatal repopulating HSCs); and adult-definitive (adult repopulating HSCs). Maturation of primitive, nucleated precursors from yolk sac in circulation has also been reported[16]. These classes of cells appeared to be generated independently of each other in distinct hematopoietic sites[17]. In other words, the origins of HSCs seemed to be multiple. Conclusions on the embryonic location of HSCs capable of long-term repopulation depended on the assays used to test them. Those from yolk sac repopulated neonate recipients better than adults, whereas those from aorta-gonad-mesonephros (AGM) repopulated adult recipients better than neonates[18]. Evidently, the successful repopulation requires a certain level of developmental compatility. After birth, bone marrow (*medulla ossea*) was proposed to be the proper niche where the formation of blood elements would continue for the lifetime as needed. Therefore, extramedullar hematopoiesis observed in liver[19,20], adipose tissue[21], cerebellar hemagioblastoma[22], meningioma[23], or subdural hematoma[24] was perceived as unusual. However, in our study, it appeared essential for tumor growth and for regeneration of normal tissues.

Erythrocytic enucleation

The debate over the mechanism leading to the elimination of the nucleus from maturing erythroblast during erythropoiesis, expulsion of nucleus or karyolysis, dated back to the late nineteenth century[25]. The current consensus on achieving enucleation by nuclear extrusion came from the ultrastructural studies published in 1967 that addressed the controversy by looking at either peripheral blood from dogs intentionally made anemic[26] or at erythroid clones grown in the spleen of irradiated mice transplanted with syngeneic marrow cells[25]. In normal peripheral blood or non-manipulated spleen, the enucleation event was too rare to study by transmission electron microscopy (TEM). Ultrastructural analysis of a developing embryo are not available in the literature, even for an organism as well studied as the mouse. The Edinburgh Mouse Atlas Project offers no TEM images (http://www.emouseatlas.org/emap/home.html). In our model, the enucleation event was frequent enough to reveal its mechanism and we found no evidence for nuclear extrusion. Instead, we observed several variants of generating erythrocytes by nucleo-cytoplasmic conversion. Thus, depending on the model, the same method could generate conflicting results. Interestingly, the analysis of chromosomal topology showed that at certain stages of erythroblast differentiation, two chromosomes were unidentifiable[27].

Below, we use the term "erythrosome" as a synonym for "erythrocyte" because the latter is not a cell.

Parallels between tumor and embryo

Similarities and differences in the antigenic composition of tumors and embryonal tissues, as well as in patterns of isozymes distribution, have been studied for years[28,29]. Reappearance in tumors of embryonic and fetal antigens, as well as isozymes, has been shown to be a common phenomenon, yet similar alterations have sometimes been observed in non-neoplastic tissues under dietary and hormonal influences[29,30]. In cases of carcinoembryonic antigen (CEA), the concept ultimately did not apply, contradicting the antigen's name, as CEA-cross-reactive antigens were located in normal human tissues including blood[31]. Also, "patterned vascular channels without EC", i.e. vascular mimicry, were observed in embryos as well as in growing tumors[32,33]. The analogy between the two types of growing tissues was further enforced by showing that tumor cells could be epigenetically reprogrammed into normal cell types[34,35]. Here, we present an unprecedented collection of original images documenting the full range of growing dynamic complexity of the tumor-induced vasculature formation, reminiscent of the embryonal one.

Definitions of stem cells

The hallmark of the classic definition of adult TSCs is the potential of the cells to self-renew and differentiate[36]. The 2002 amendment to that definition[37] emphasized additional aspects of the concept, namely: a shift from the cellular view to a system view including self-organizing processes, stemness as a capability rather than as a cellular property, dependence on the growth environment, within-tissue plasticity, and the functionality of the TSCs and the tissue. The stemness as an attribute of a system, rather than of a particular cell lineage, questioned the usefulness of presumed protein markers for identifying stem cells (SCs)[37–39]. With regard to both embryonal and cancer SCs (ESCs and CSCs, respectively) the views remain opposing. On the one hand, neither ESCs nor CSCs fulfill all those criteria[40]; on the other hand, both do but with certain qualifications. In the case of the ESCs, self-renewal and differentiation is likely to occur sequentially for two reasons. (1) The redundancy during development could serve as an evolutionary safety measure; in the context of the early embryo, that could mean generating a certain number of identical cells before their differentiation begins[41]. (2) Heterogeneity with respect to cell cycle activity was detected even in such an iconic cell lineage as the HSCs of adults[42]. In case of the CSCs, their role in tumorigenesis appeared to depend on microenvironment as discussed below and in one of our accompanying articles[43].

The goal and significance of this study

The goal of our study was to visualize the cellular mechanisms of vasculature formation associated with the growth of malignant tissue. We carried out the ultrastructural *in situ* analysis of initially avascular breast tumor spheroids co-implanted with homologous tissue graft, into the mouse dorsal skin folds[44,45]. A complementary study on such spheroids implanted without the graft is the subject of a separate report[43]. In contrast to the reductionism that dominated the ultrastructural studies of the second half of the last century, we analyzed tissue sections instead of isolated tissue components. The high resolution was necessary to investigate distinct physiology and

functions of individual cells whereas the tissue context unveiled interactions among the cells. The results revealed interdependence between erythrogenesis and vasculogenesis localized at the site of tissue growth or repair and other new qualities of the emerging system. The data illustrated a great variability and increasing complexity of the vasculature morphogenesis, i.e., formation of blood and vessels, as both were evolving from primitive forms while enabling the tissue building process. Like in the embryo[17], the new tumor vasculature was developing independently of the existing one. New erythrosomes and other blood elements formed extramedullary, and new vessels were assembling around them before initiation of the blood flow occurred. Vessel "sprouts" progressed toward other vessels not away from them. By suggesting local tissue cells as progenitors of the new vasculature, those observations related to the concept of tissue stem cells (TSCs).

The results of the morphological analysis of the vasculature formation in our model were consistent with the amended functional definition of the TSCs concept. They are not in harmony with the common understanding of the cell lineages as hierarchical and irreversible progress of differentiation. Moreover, the new findings suggest a hypothesis that the adult vasculature formation represents a partial recapitulation of the embryonal organogenesis involving coordinated activity of some cells capable to form all tissue types of a particular organ *de novo*. Such a perspective is not entirely new. The term "organoblast" was used in 1997 in reference to pediatric salivary gland tumors that had morphological characteristics of the organ with maturation arrested at a primitive state of development[46]. Later, mouse mammary SCs in the form of *in vitro* grown mammospheres ("organoids") were shown to regenerate morphologically normal mammary epithelial ducts after implantation into mammary fat pads surgically cleared of the endogenous epithelium[47].

Our results also demonstrate the potential of immunocytochemistry to reveal further molecular-level details of the cellular interactions as they relate to regional tissue growth. This approach is suitable to validate concepts derived from proteogenomics as well as effects of pharmacological treatments. It is far more relevant to medical problems than *in vitro* studies and cheaper than conducting clinical trials.

Materials and methods

The study was performed according to protocols approved by Sidney Kimmel Cancer Center's (SKCC) OLAW-approved Institutional Animal Care and Use Committee (Assurance No A4128-01). The protocol numbers were: 03–16A and 05–11 for Grants CA104898 and CA119378, respectively. No human specimens were involved in any of the experiments outlined here.

Acronyms

AGM: aorta-gonad-mesonephros
ATP: adenosine tri-phosphate
BMP4: bone morphogenetic protein 4
CEA: carcinoembryonic antigen
CIB1: calcium & integrin binding protein 1
CSCs: cancer stem cells
ECM: extracellular matrix
ECs: endothelial cells

ER: endoplasmic reticulum
ESCs: embryonal stem cells
GFP: green fluorescent protein
H2B: histone 2B
HSCs: hematopoietic stem cells
OLAW: Office of Laboratory Animal Welfare
RT: room temperature
SCs: stem cells
TEM: transmission electron microscopy
TIMPs: with tissue inhibitors of metalloproteinases
TSCs: adult tissue stem cells
VVOs: vesiculo-vacuolar organelles

Animals
Host and graft donor, female, athymic nude mice, 8–9 weeks old, were purchased from Harlan. The donor mouse with GFP-labeled ubiquitin was from The Jackson Laboratory (Stock Number: 004353; Strain Name: $C_{57}BL/6$-Tg(UBC-GFP)$_{30}$Scha/J). The mice were housed in the SKCC animal care facility with controlled 12/12 hr light/dark cycle and temperature maintained at + 22°C. The mice were on Tekand global 14% protein rodent diet (Harlan) with access to water ad libitum. For surgery, they were anesthetized (7.3 mg ketamine hydrochloride and 2.3 mg xylazine/100 g body weight, inoculated i.p.) and placed on a heating pad. Immediately before tissue harvesting the tumor hosting mice as well as the graft donors were euthanized with pentobarbital overdose (100 mg/kg i.p.).

Cell lines
The parental murine breast cancer cell line, N202.1A[48] was stably transfected to express GFP under histone H2B promoter[49]. The two cell lines, N202.1A parental and N202.1A+H2B-GFP (obtained from Drs. J. Lustgarten and P. Borgstrom) were used to form tumor spheroids by culturing 2×10^5 cells per well for 2–3 days prior to implantation.

Chambers
A week after establishment of mouse dorsal skin chambers, the tumor spheroids were implanted on a pad of homologous tissue, namely, minced breast fat pad from a lactating mouse (pseudo-orthotopically) as described earlier[45]. The tumors were incubated in the chambers for one or three weeks (Table 1). Their final size was about 1–3 mm in diameter. The blood circulation in tumor vessels was monitored *in vivo* by light microscopy before disassembling the chambers[50].

Antibodies
The GFP-specific rabbit polyclonal IgG (ab290) was from Abcam; CIB1-specific rabbit polyclonal IgG (11823-1-AP) was from ProteinTech Group, Inc.; CD34-specific rat monoclonal IgG$_{2a}$ (sc-18917) and non-reactive goat polyclonal IgG (sc-34284) were from Santa Cruz.

Tissue processing
The tumors with some surrounding tissues were dissected out and cut in halves perpendicularly to the host skin surface while immersed in cold fixative (4% paraformaldehyde in 0.1 M Na cacodylate pH 7.4). The skin region served later as a reference to distinguish between edges of the tumor facing the skin and those facing the glass window of the chamber. The halves were then separated and processed independently for TEM and immunocytochemistry.

TEM
The tissues were transferred into a stronger fixative (4% paraformaldehyde/2.0% glutaraldehyde in 0.1 M Na cacodylate pH 7.4) to better preserve the ultrastructures before further cutting. They were cut into 1 mm thick slices in planes perpendicular to the plane of the first cut and to the skin surface, finally, into ~ 1 mm³ blocks, transferred into a fresh portion of the fixative in which they were cut and incubated for 2 hrs at 4°C. The fixed tissue blocks were washed with 0.1 M Na cacodylate – HCl buffer pH 7.4 (3 × 15 min.) and post fixed in 1% OsO_4 in 0.1 M Na cacodylate buffer, pH 7.0 for 60 min. on ice, washed with water and stained with 1% uranyl acetate at room temperature (RT) for one hour. The blocks were embedded in EMbed-12 (EM Sciences, Cat. No 14120). The resin embedded tissues were cut into 60 nm sections, using a Leica Ultracut UCT ultramicrotome, and stained with lead citrate[51] or viewed without further contrasting.

Immunocytochemistry
During cutting into ~1 mm³ blocks as described above, the tissues were kept in the mild fixative to protect antigenic epitops (4% paraformaldehyde in 0.1 M Na cacodylate pH 7.4). The tissue blocks were vitrified by infiltrating the pieces with 50% PVP (polyvinylpyrrolidone) containing 2.3 M sucrose in 0.1 M Na-cacodylate buffer, pH 7.4, for 2 hrs or over night, mounted on metal pins and frozen in liquid nitrogen, as described by Tokuyasu[52]. Frozen tissues were cut into 70 nm sections, using a Leica Ultracut UCT ultramicrotome with the cryo-attachment. The sections were picked from the knife with 2.3 M sucrose and floated on 1% ovalbumin (Sigma, Cat No.A5378) in 0.1 M Na-cacodylate buffer for at least one hour before incubation with specific or non-reactive antibody (50 µg/ml) at RT for one hour. Sections were then rinsed eight times with 0.1% ovalbumin in the same buffer and incubated for one hour with 10 nm Au coupled to protein A (from Dr G. Posthuma; Cell Microscopy Center, university Medical Center Utrecht, The

Table 1. Experimental design.

Figure numbers	Host mouse no	Tumor cell line	Graft tissue	Incubation time (days)
1, 4 (A-D & F), 5 (A, B, E, F), 6, 7 & 15 (A, B)	5 (hyaline membrane)	N202.1A parental	Ubiquitin-GFP breast fat pad	5
2, 3, 4 (E & G-I), 5 (C, D) & 8 (A-H), 15 (C-F)	5	N202.1A parental	Ubiquitin-GFP breast fat pad	5
9, 10 (C), 15 (C)	3	N202.1A+H2B-GFP	Breast fat pad	22
10 (A, B), 11–14, 15 (D, E, F)	2	N202.1A+H2B-GFP	Breast fat pad	21

Netherlands). The eight rinsing steps were repeated before fixation of the immune complexes with 1% glutaraldehyde. After rinsing three times with water, the immunostained cryosections were contrasted with a mixture of uranyl acetate and methyl cellulose (25 centipoises, Sigma M-6385) in water, at a final concentration of 1.3% each, for 10 min. Excess liquid was removed and the sections were dried at RT.

Viewing

All sections were viewed and the images captured at 100 kV using a Morgagni 268 electron microscope equipped with MegaView III digital camera. Analyzed tissue sections were first examined at low magnification and coordinates for each hexagonal sector of a grid covered with tissue were recorded automatically. Subsequently all sectors were explored at least once at variable high magnifications. Interesting images were captured at the magnification best suited to document a particular phenomenon or structure, including colloidal Au grains. The images were transmitted from the microscope camera to an iTEM imaging platform from Olympus Soft Imaging Solutions and archived in a designated database. In some cases, the final images were assembled by multiple image alignment (MIA) to increase the surface area without losing the resolution. We used the graphics editing program, Adobe PhotoShop, to add cell type-specific color-coding shown in the twin set of images included in the Supplement.

Experimental design

Three of the five recipient mice used in this and two accompanying articles were assessed here, as summarized in Table 1. The same numbering system was used in all three articles. The other two mice had the tumor spheroids implanted without the graft. The same numbering system was used in all three articles. Three weeks after implantation, we observed a range of stages of vasculature formation simultaneously due to continuous growth of the tumors. Cells responding to locally variable microenvironment were not synchronized. We added the five days incubation time to see if other time points were necessary to extend that range. Indeed, different yet overlapping sets of options were found. However, between the two types of implantation, with & without the graft, the range of options for tumor supporting vasculature formation was well represented three weeks after implantation. Therefore, we concluded that additional time points were not necessary for our purpose. Yet, it was at the short incubation time that the hyaline membrane between the tumor & the glass remained unattached to the underlying tissues. That fragile membrane collapsed into a viscous droplet on the glass wall of the chamber at the time of tissue harvest and was analyzed because it appeared to contain a red, vascular pattern-resembling network when viewed through dissecting microscope lenses. Images from the hyaline membrane introduced additional observations regarding morphogenesis of the fibrous tissue on top of the implanted tumor, including vasculature formation in the non-malignant tissue.

Results

Multiple steps of cellular differentiation and the growing complexity of the vasculature formation process were observed in tissue samples harvested at only two different time points (5 and 21 days after implantation) due to local variability resulting from lack of synchronization *in vivo*. The emergence of increasingly more specialized phenotypes of individual cells characterized those steps,

signifying progress in the cellular differentiation. Multiple forms of erythropoiesis reflected the multiple levels of cell maturation.

Five days after implantation, in hyaline membrane between the tumor surface and the glass chamber wall, the earliest event seen was migration of megakaryocytes and erythroblasts and their products, platelets and primitive erythrosomes respectively, along with the bipotent precursors of both cell types[7,53–55] (Figure 1 & Figure S1). The cells seemed loosely bound together by fibrous (non-collagen) secretion, likely proteoglycans. They appeared to be migrating in columns and differentiating simultaneously, as if scouting the hypoxic avascular space under the glass and establishing a blueprint for vascular pattern. A composite dense body resembling those seen in platelets[56] was found in one of the cells depositing elements of ECM (Figure 1 [E & F]) and suggested that the cell building ECM was related to the cell type producing platelets, i.e., to megakaryocyte. At the same time on the tumor surface, the two cell types had formed a primitive vascular pattern in the absence of ECs (Figure 2 & Figure S2). A crystalline inclusion resembling an Auer body[57] was found in a small structure of such nature (Figure 2 [C]). The formation of vasculature attached to the tumor was similar to that of tumors incubated for three weeks without the graft (Figure 1 [D] in the accompanying article II). That similarity represented an overlap in terms of the earliest stages of vasculature morphogenesis found at incubation times two weeks apart. In both cases, the cells represented two principal functional attributes of the vasculature. The first attribute, the metabolism-related functions of transporting gases (O_2 & CO_2) and of generating ATP anaerobicly[58], were associated with erythrosomes. The second one, the structure-organizing functions, were represented initially by pro-megakaryocytes in the form of secreted elements of the extracellular matrix (ECM), possibly carcinoembryonic antigen (CEA)[31] and later, by mature megakaryocytes and platelets. That way, megakaryocytes were in a position to receive additional nourishment (ATP) from the erythrosomes as their mitochondria suffered from some hypoxic distress (Figure 1 & Figure S1 [F]). ECs were absent. By shaping the vascular pattern, megakaryocytes presented themselves as a cell type involved in early vasculature morphogenesis, in addition to the known later role of platelets in mending vascular injuries by their aggregation and the thrombus formation. At higher magnification, the emerging erythrosomes revealed nucleo-cytoplasmic conversion as the mechanism of enucleation in single erythroblasts as well as in clusters of them (Figure 3 & Figure S3).

The immunohistochemical staining detecting CD34 confirmed the erythropoietic lineage identity of the cells by analyzing frozen counterparts of the samples shown in Figure 1, Figure 2, Figure 3 & Figure S1, Figure S2, Figure S3 (Mouse 5, and some from Mouse 3). The CD34 label was present in mononuclear and giant polyploidal erythroblasts (Figure 4 & Figure S4 [A-F] & [G-I] respectively). Both types were at the early stage of nucleo-cytoplasmic conversion but in the giant cells, the mitochondria were still intact and they were oversized. The few giant cells belonged to a larger cluster of such cells, most likely representing cells undergoing growth and endoreduplication before converting into giant erythroschizonts that would later break into erythroschizomers. Together those features suggested very efficient production of large number of erythrosomes. In 1909, Maximow interpreted the emergence of such extremely
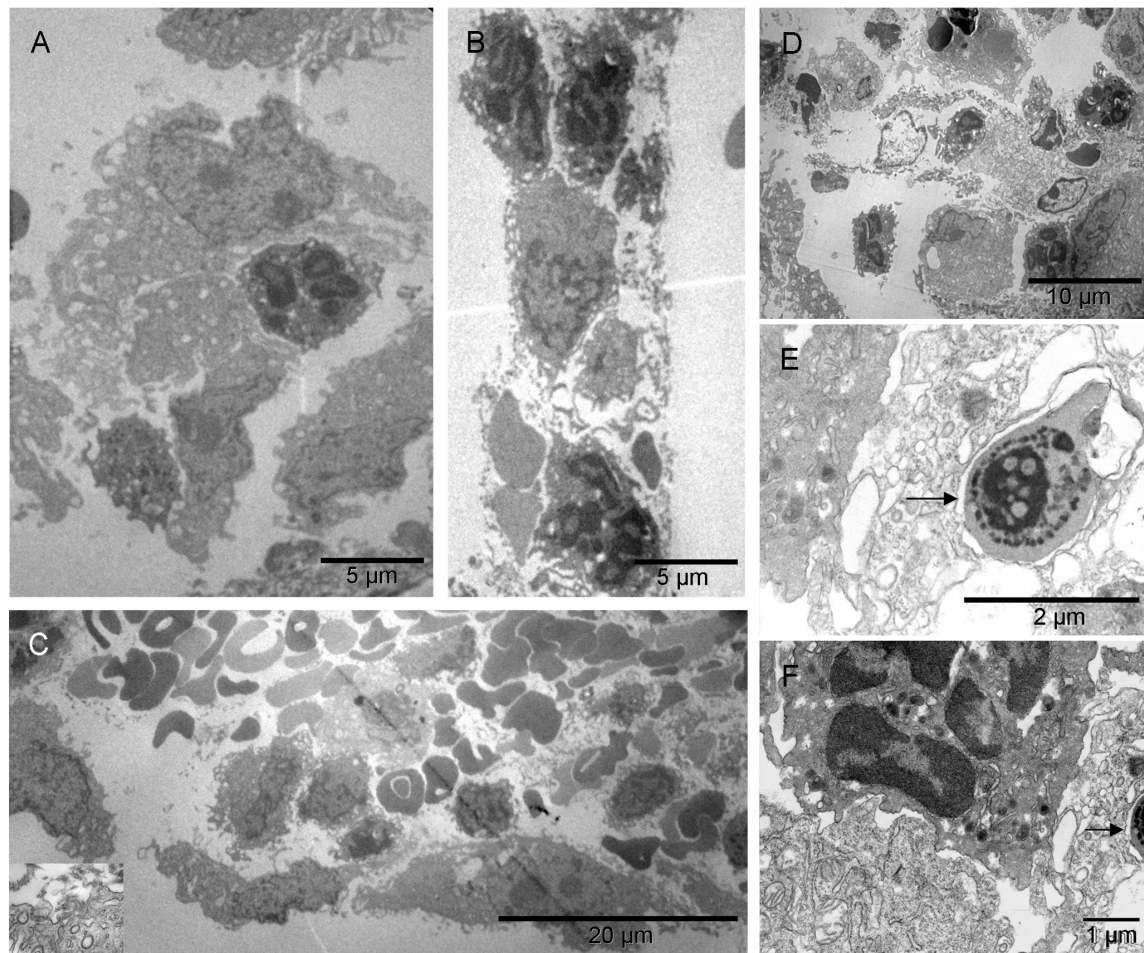
Figure 1. A blueprint for vascular pattern created by migrating erythroblasts and megakaryocytes. The pattern-forming heterogeneous population of the cells migrating in the hyaline membrane consisted of (a) those with large nuclei occasionally containing double nucleoli and with asymmetrically distributed, irregularly shaped, large cytoplasm and satellite platelets i.e. megakaryocytes, and (b) those with atypical, lobular, heterogeneously dark nuclei and dark cytoplasmic granules in the absence of mitochondria, usually accompanied by erythrosomes, i.e. most likely erythroblasts [**A**]. The four elements, cellular and sub-cellular (erythrosomes and platelets), appeared evenly dispersed among each other like in the narrow (about capillary short dimension) column in [**B**] or the megakaryocytes that displayed a tendency to migrate to the periphery of the larger cluster and surround the other elements [**C**]. Those poorly differentiated cells were probably bipotent, megakaryocyte and erythroid, progenitors [**C**]; compare with Figure 8 in[55]. The cellular and sub-cellular elements appeared to be held together with extracellular fibrous components, possibly proteoglycans and little collagen (the insert in [**C**]). The resulting red pattern appeared as a vascular network under low magnification of dissecting microscope. The parallel arrangement of extracellular, short, non-collagen fibers suggested mobility for the cells secreting them [**D**]. The extra-cellular matrix (ECM) producer [**E**] located to the right of the erythroblast [**F**] contained a composite dense body (arrows in [**E** & **F**]) characteristic of platelets (Figure 111-1, E in[56]).

large primitive nucleated red cells found in mammalian embryos as a response to relative hypoxia of the fetus and the need for rapid generation of a large amount of blood[13]. The extramedullar erythropoiesis induced by hypoxia of growing tumors resembled fetal erythropoiesis in that regard.

Detecting the green fluorescent protein (GFP) label of either the graft or the tumor spheroids helped to address the question of the source of hemato-vasculogenic cells in the tumor microenvironment. In Mouse 5, the graft tissue originated from the donor mouse that carried the GFP marker under a ubiquitin promoter. Thus the GFP label found in erythroblasts, erythrosomes, platelets and ECs indicated participation of the graft cells in building of the tumor vasculature (Figure 5 & Figure S5), although unlabeled cells with similar morphology were also present. Cells with ambivalent morphology, like the one in Figure 5 & Figure S5 [F], provided a hint that ECs were evolving from erythroblasts.

We wondered if a mechanism similar to the one controlling hemostasis could play a role in establishing the vascular pattern before forming the endothelium. A protein best known for its involvement in platelet aggregation and thrombus stabilization, calmyrin,
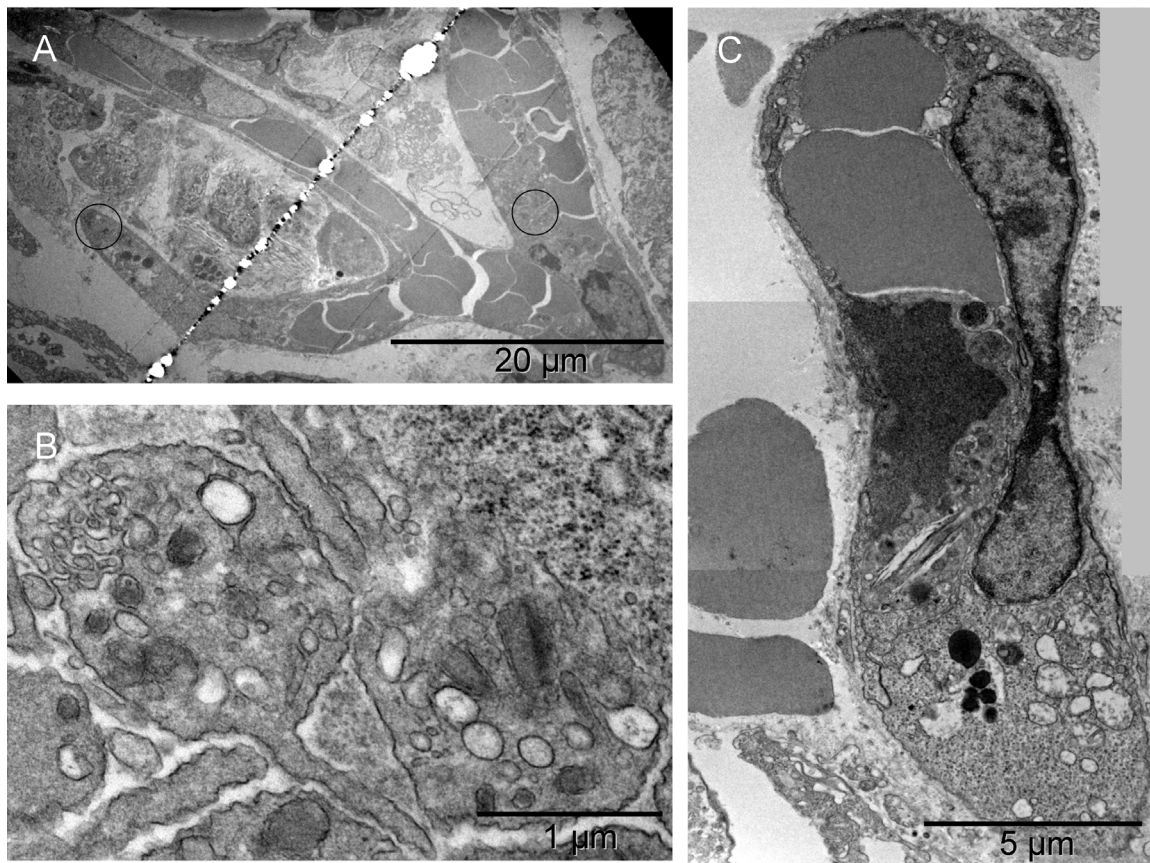
Figure 2. Primitive vascular pattern formed by megakaryocytes without endothelium. Primitive vascular pattern in the tumor-harboring solid tissue below the hyaline membrane consisted of megakaryocytes and platelets engaged in direct and tight contact with one another and with erythrosomes and erythroblasts. There were no ECM-filled spaces left between them nor was there an additional cellular layer covering those elements. The elongated branching structure in [**A**] appeared kept together by megakaryocytes and platelets (N.B. the line in the middle of the image is a scratch caused by an imperfection of the knife-edge during cutting the section). In the two circled regions of that structure, incomplete separation of platelets from megakaryocytes provided ultrastructural evidence for their identity and for an ongoing process of generating platelets at that location. One region was the bifurcation area at the base of the right almost vertical branch, enlarged in [**B**] and the other was the tip of the lower left branch (enlargement not shown). Evidently, megakaryocytes were capable of organizing erythrosomes into branching primitive vascular structure before ECs emerged to provide protective walls of a vessel. In a smaller elongated structure of similar nature, although without platelets in the section plane, one of the cells contained an Auer body [**C**], previously described in neutrophils from cases of leukemia and defined as azurophilic, large, elongated granules (Figure 64-10 in[57]). The upper part of that cell contained two erythrosomes; whereas what remained of the nucleus had a different texture compared with that of the nucleus in the second cell of that complex. The prominent dark granules of the latter resembled those in the cell next to the megakaryocyte from the tip of the lower branching structure in [**A**]. If the irregularly shaped seemingly empty space next to those granules was a prototype of a lumen then both those cells could have potentially been angioblasts.
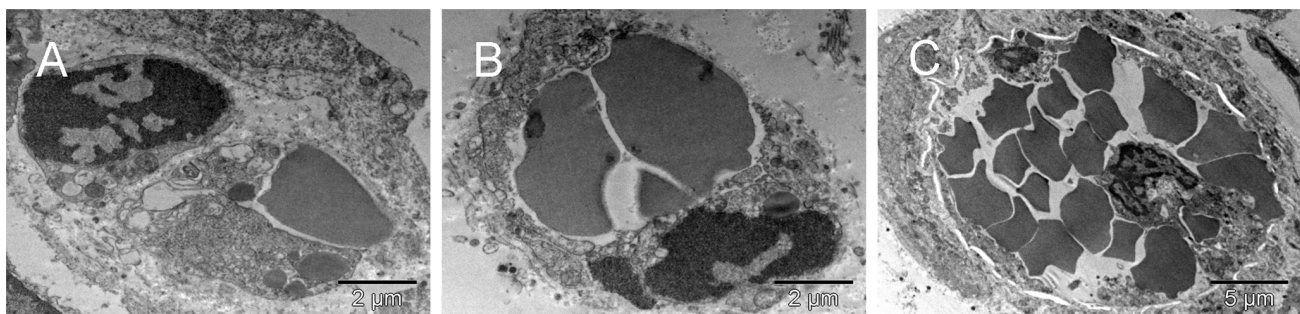

Figure 3. Extramedullar erythropoiesis via nucleo-cytoplasmic conversion. The single cells undergoing structural remodeling in the nucleus and cytoplasm [**A** & **B**] represented at slightly different stages of erythropoiesis. Conceivably, a few such cells, when gathered into a cluster, could fill up a larger space with erythrosomes creating a cobble stone pattern, also called 'erythropoietic lake' or myeloplaxes [**C**]. Platelets and megakaryocyte were recognizable at the periphery of the cluster.
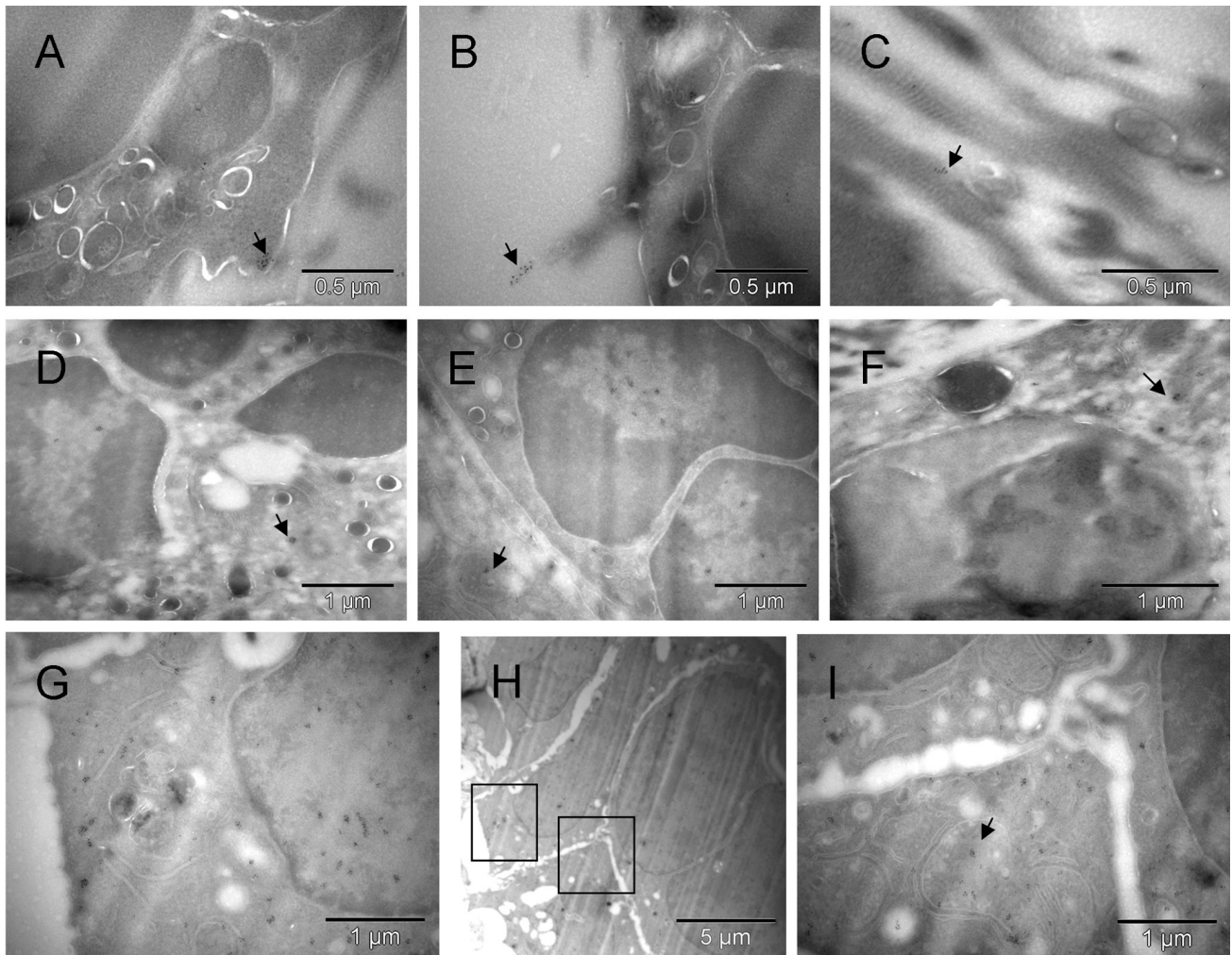
Figure 4. HSCs and their progenitors at the tumor site labeled with CD34 marker. Clusters of the gold label were found on the cell surface, in the nucleus, cytoplasm and mitochondria of cells morphologically fitting the description of erythroblasts [**A**, **B**, **D** & **E**] and on extracellular collagen fibers produced by them [**B** & **C**]. A fragment of cell with mixed phenotype is shown in [**F**]. The cluster of CD34-labeled giant erythroblasts (potentially leading to myeloplaxes) contained one cell with a double nucleus (right side in [**H**]). Two regions of [**H**] are enlarged in [**G** & **I**], left and right respectively, to show oversized mitochondria, some converting into peroxisomes [**G**]. That cluster of cells was bigger than the one shown earlier (Figure 3C), and the presence of mitochondria despite clear commitment to erythrogenesis suggested that here the process was more efficient. Arrows point out some clusters of Au grains.

also known as calcium and integrin-binding protein (CIB1), was therefore detected next. Consequently, a new role for calmyrin in tissue morphogenesis emerged from such analysis of the hyaline membrane where the cells were mostly separated from one another. At low magnification, occasionally triplets of cells were seen within a single field; each one with different features that suggested that they were related but currently committing to become either megakaryocytes, erythroblasts or ECs (Figure 6 & Figure S6 [A, B & C] and Figure 7 & Figure S7). The calmyrin-specific label was located in all three morphologically distinct cells and in the fibers connecting the differentiating ECs with another cell and in the ECM (Figures 6 & Figure S6 [C & D] respectively), as well as in large, possibly polyploidal cells that contained internal vesicles similar to those in the cells of regular size (Figure 6 & Figure S6 [D & G]). Those vesicles were either becoming erythrosomes or losing their electron-dense

content. The cells were perishing in the process but at the same time, they were changing the microenvironment by leaving traces of their presence in the ECM as developmental clues for other cells. All that suggested that the differentiation process was happening there by means of trial and error, i.e. cytoevolution. Calmyrin seemed to be instrumental in building this tissue canvas. Overall distribution of the protein inside the cells was compartmentalized (Figure 6 & Figure S6 [E, F & I]) but within each compartment, the calmyrin label was dispersed randomly. Inside the primitive erythrosomes of the hyaline membrane, the label was also dispersed (with rare exceptions), unlike in those from the solid tissue closer to the tumor.

In those more differentiated cells beneath the hyaline membrane, the calmyrin-specific label formed clusters over an area of about caveolar size, i.e. 70 nm in diameter (Figure 8 & Figure S8) revealing
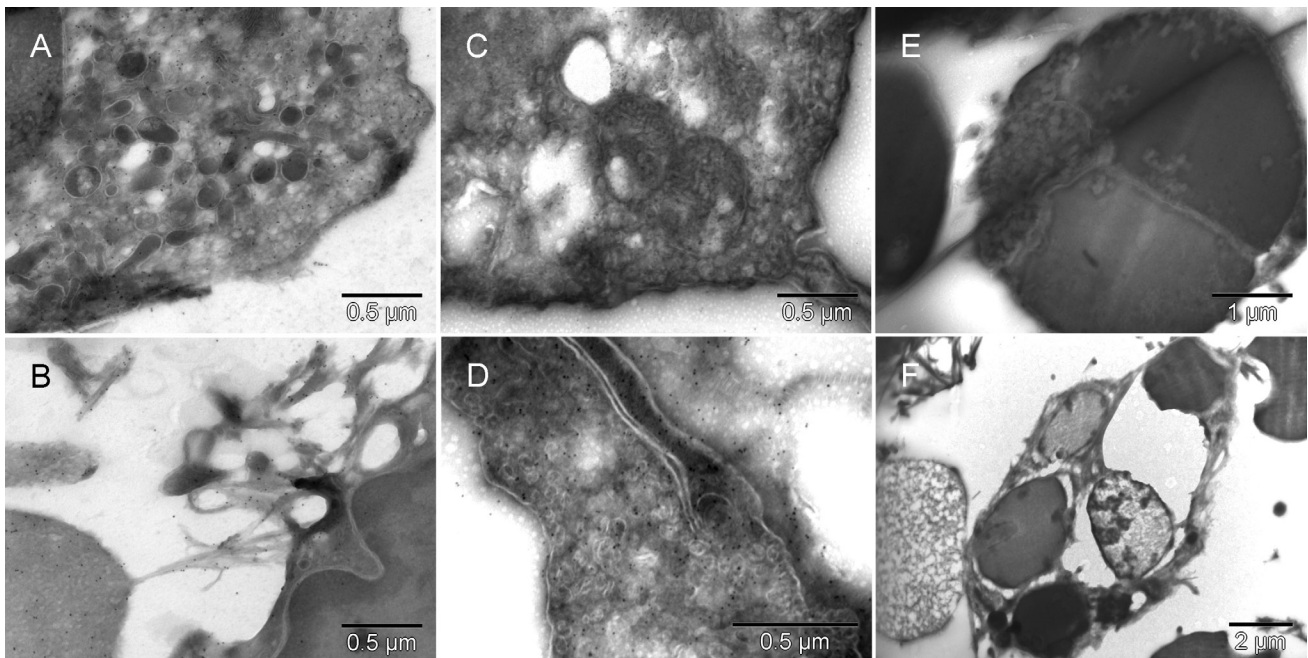
Figure 5. Cells of graft origin labeled with GFP under ubiquitin promoter. GFP-specific label was present in erythroblasts [**A**], primitive erythrosomes like the one separating from the cell that made it (left lower corner in [**B**]), platelets [**C**] and in EC [**D**]. Morphologically interesting cells, erythroblast [**E**] and perishing hemangioblast [**F**], stained with nonspecific antibody are shown at low magnification (they had no gold grains). The erythroblast was entirely consumed by a successful incremental conversion into at least three erythropoietic vesicles [**E**] and the cell with ambivalent phenotype [**F**], possibly hemangioblast, contained three internal vesicles resembling erythrosomes and two of comparable size that appeared to be failing as erythrosomes (partially electron lucent ones).

a new ultrastructural element, the calmyrite. The sub-cellular location of the calmyrites in mitochondria, peroxisomes and erythrosomes, suggested that all three of those organelles were homing previously unreported ultrastructural elements related to energy metabolism. In addition to cell types shown in Figure 8 & Figure S8 [A–H], calmyrites were seen in megakaryocytes, platelets, granulocytes, plasma cells, smooth muscle and rat normal EC(s). The included rat lung section (Figure 8 [I]) demonstrated that calmyrites existed in normal differentiated cells together with mitochondria and were not a product of necrotic process, but rather representing a backup metabolic pathway rendering robustness to the cellular metabolism.

Three weeks after implantation, some cells kept converting into the erythrosomes and others kept providing structural support to them but in a more complex way. Their phenotypes kept changing (Figure 9 & Figure S9). Some cells were producing large amounts of collagen as if converting their entire cytoplasm into masses of collagen while their nuclei were converting into erythroschizosomes (Figures 9 & Figure S9 [C]) leading to a new tissue canvas in the form of fields of collagen with erythrosomes scattered in there. Such vessel-free erythrosomes described earlier in a similar context were believed to be extravasated erythrocytes. Eosinophils, adipocytes and dendritic cells were occasionally present in that environment as well. Erythrosomes and cells providing structural support to them seemed to have been chemotacticly attracted to each other regardless of the current level of their differentiation. Moreover, segments of new vasculature with increasing structural complexity were assembling around emerging erythrosomes into

capillaries and vessels of variable size simultaneously. Occasionally, megakaryocyte-resembling cells were positioning themselves like pericytes, i.e. abluminally, close to a forming vessel. The one in Figure 9 & Figure S9 [B] might have been a megakaryocyte evolving into ECs or pericyte. Still greater complexity of the vasculature morphogenesis was evident in the second mouse with tumor grown for three weeks. Depending on the location in the section, the more primitive forms of the vasculature were present as well. Collagen came across as an important factor for building not only vasculature but also tumor tissue (Figure 10 & Figure S10). Signs of hypoxic stress were in the form of relatively small darkening or necrotic mitochondria (loosing their internal structure) and dilated cisternae of endoplasmic reticulum (ER) partially depleted of ribosomes and resembling vesiculo-vacuolar organelles (VVOs)[59], (Figure 10 & Figure S10 [D]).

Arteries and veins were formed independently, each vessel type from individual, differentiated cells. The level of differentiation varied. The two shown arteries assembling from differentiated cells of variable type (including chromaffin cells) would have likely joined eventually had the tissue been harvested later (Figure 11, Figure 12, Figure 13 & Figure S11, Figure S12, Figure S13).

Moreover, developing nerves accompanied some forming vessels (Figure 14, Figure S14, and Figure 15 & Figure S15 [D & E]). One displayed a few nerve fibers at early stages of myelination and a lack of mature synapses despite the presence of multiple nerve boutons with synaptic vesicles. Next to it, an equivalent number of cells committed to the erythropoietic pathway generated a giant
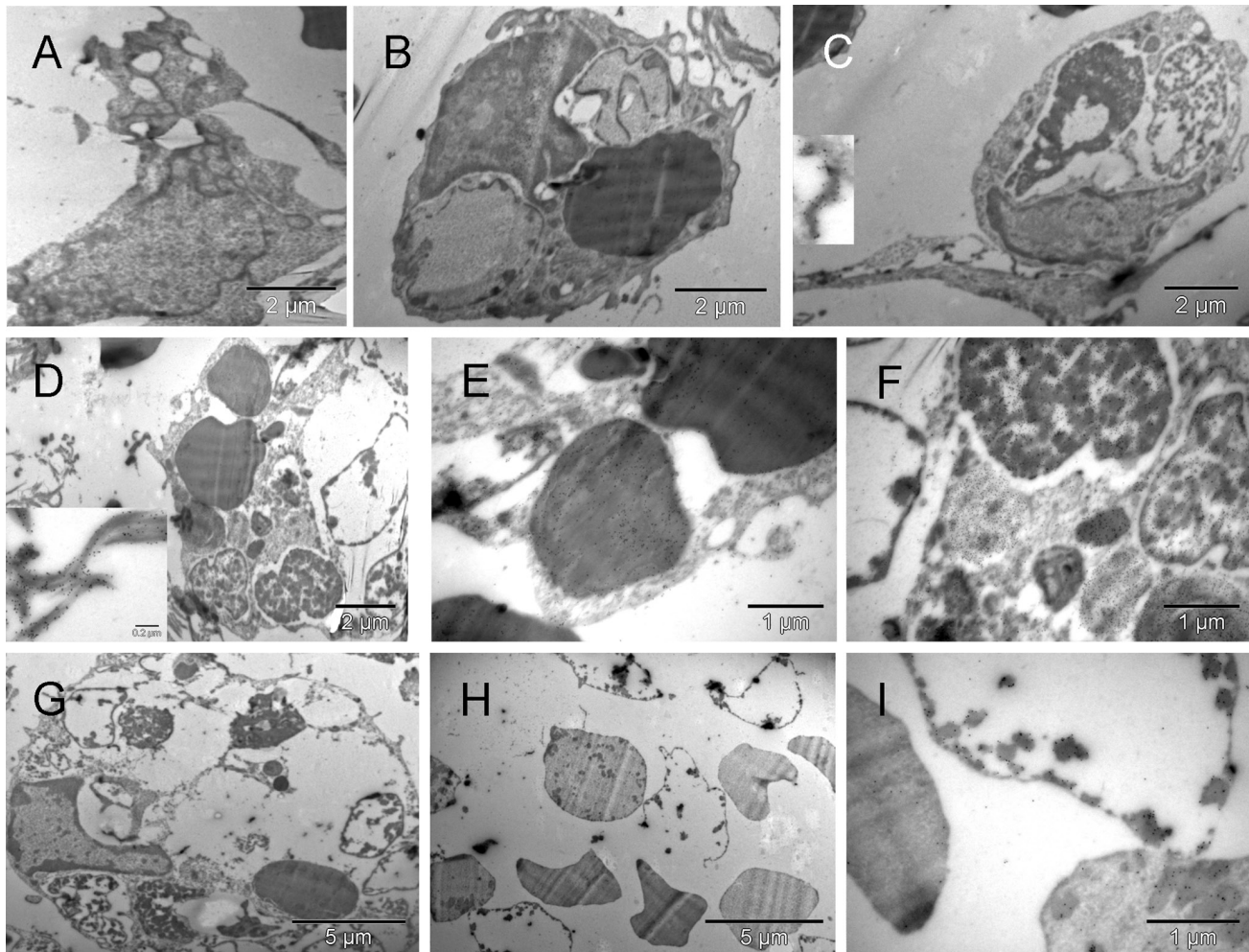
Figure 6. HSCs differentiation by evolution. The cells shown in the upper row [**A**, **B** & **C**] were located in the hyaline membrane 5 µm (or less) apart from one another (Figure 7 & Figure S7) suggesting their relatively recent derivation from a common precursor. The first, irregularly shaped cell with platelet-resembling attachment was probably a megakaryocyte [**A**]. The second one, had four large vesicles but only one of them was similar in size and electron density to a cell-free erythrosome (right upper corner in [**A**] and elswhere), whereas two other vesicles were much lighter with the exception of small patches at the periphery, and the fourth one was probably an incompletely converted nucleus [**B**]. The third cell had two large vesicles and both appeared to represent different stages of degradation of the material they were made of [**C**]. The outer membrane of that cell was at one side connected to another cell via calmyrin-containing extracellular fibers (insert in [**C**]). Both cells with the large vesicles made impression of cells with mixed phenotypes with some inclinations to specialize in either producing erythrosomes [**B**] or forming a lumen [**C**]. Fields shown in [**D**–**I**] were in the same section; they represented what seemed to be left after internal remodeling of polyploidal cells or multi-cellular clusters [**D** & **G**]. There were cell-free erythrosomes as well as empty vesicles, some broken [**H**]. Clearly, cells were perishing because of such restructuring but they were also changing the microenvironment. Insert in [**D**] shows calmyrin-specific label on fibers of ECM. [**E**, **F** & **I**] are enlarged regions from [**D**] and [**H**], respectively.

erythro-schizosome, although perhaps normally there would have been a cluster of erythrosomes ("erythropoietic lake") in a forming vessel. Whether this particular one was going to be successful in producing normal erythrosomes or was just a part of the ongoing cytoevolution was not clear. The cells that surrounded the developing nerve did not necessarily derive from the ectoderm. They ended up on the surface of neuroplax but had much in common with endothelium, morphologically and functionally – namely, a flattened shape, plenty of caveolae to control the microenvironment of the developing neurons and Schwann cells. Caveolae were shown elsewhere to contain ATP-ase that could be processing ATP secreted by the giant erythroschizont right next to it[60–63]. Such concerted differentiation resulting in different functions would have been unlikely to happen without coordinated regulation of the vasculature and nerves.

In summary, the observed variants of erythrogenesis included nucleo-cytoplasmic conversion and nuclear conversion with collagen
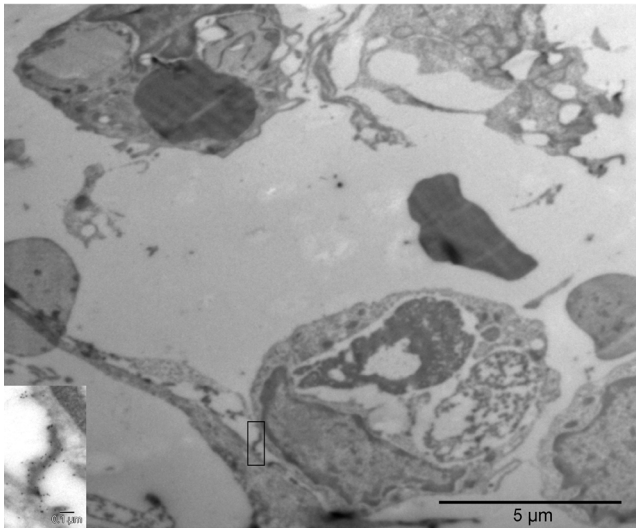
Figure 7. Relative location of megakaryocyte, erythroblast and ECs precursors *in situ*. Compare with Figure 6 [A,B & C]. The insert shows calmyrin-containing extracellular fibers connecting the adjacent cells.

production continuing in the cytoplasm. Erythroblasts were either entirely devoted to erythrogenesis or had ambiguous phenotype, including electron lucent (failing) vesicles, collagen synthesis and later also presence of caveolae. Erythrogenic conversion affected entire cells or syncytium and later generated schizomers (myeloplaxes, cobble stone areas, erythrocytic lakes) or the cellular remodeling occurred incrementally. Erythroblasts had aerobic or anaerobic metabolism as indicated by the presence or absence of mitochondria. They were polynuclear or mononuclear and of giant or average cell size. The erythrosomal membrane was or was not undergoing remodeling inside the erythroblast before release of the organelle. Some cells were perishing without succeeding in production of either proper erythrosomes or a lumen despite initiating those processes. Evidently, the cellular differentiation was happening by means of natural selection (cytoevolution). Cells perishing in the process were contributing to building tissue framework available for subsequent remodeling. Erythropoiesis appeared to be essential at every step of evolving cellular mechanisms of vasculature formation. Fusion of the neo-vasculature with the pre-existing one would be the final step needed to allow the newly created portion of tumor tissue, already equipped with its own vasculature (a network of blood-containing vessels of variable size), to grow beyond the limit set by
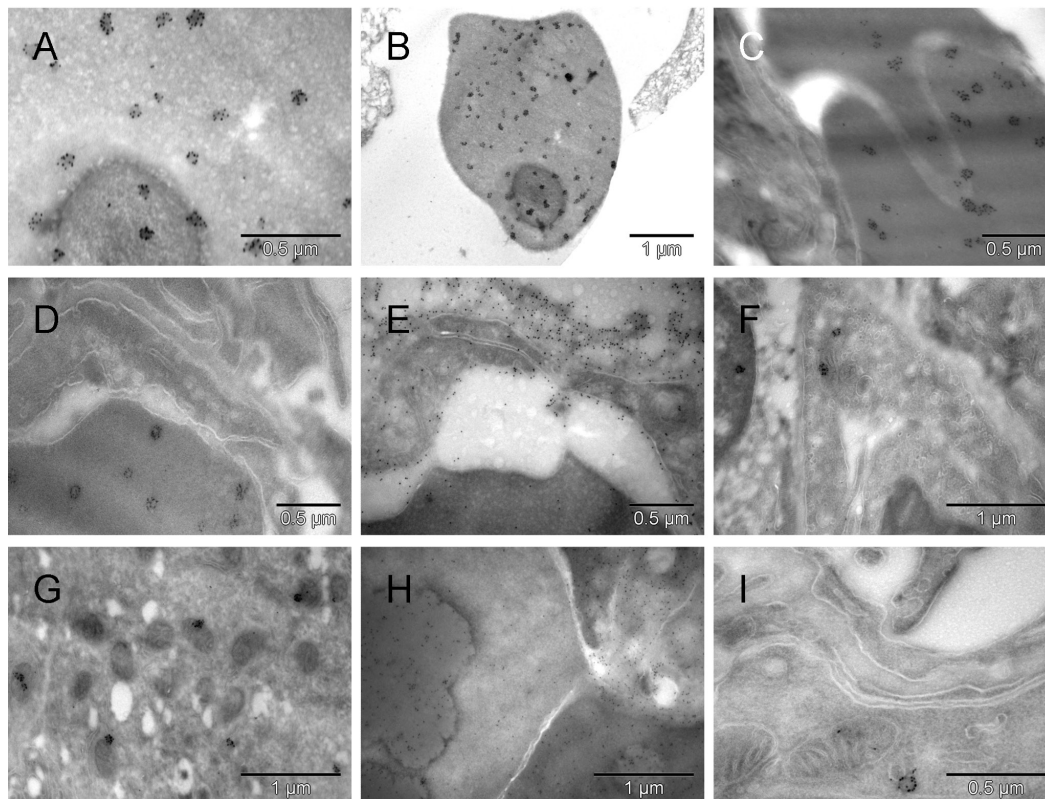

Figure 8. Calmyrite: a new ultrastructural entity involved in anaerobic metabolism. Uneven distribution of the abundant calmyrin-specific label in erythrosomes from the solid tissue under the hyaline membrane was striking [**A**, **B**, **C** & **D**]. No such clusters were seen extracellularly [**E**]. The gold particles appeared arranged with certain symmetry in clusters of about 6 to 12, as if the protein became a part of distinct para-crystalline ultrastructures that in less differentiated regions were not formed ([**E**] and Figure 6 & Figure S6). Such gold grain clusters were also present in ECs [**F**] and tumor cells [**G**] where small dark mitochondria suggested hypoxic distress. In a giant cell the uneven distribution of scattered calmyrin-specific label and heterogeneity of electron density indicated an ongoing process of erythrogenic conversion [**H**]. One calmyrite in a section from normal rat lung is shown in [**I**]. Those ultrastructural para-crystalline elements visualized by calmyrin-specific label are being described here for the first time and referred to as calmyrites.
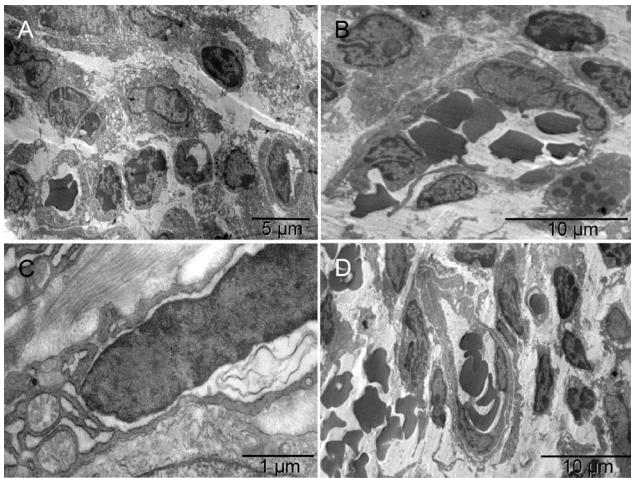
Figure 9. Progress in cellular differentiation and assembly of new vessels. Three weeks after implantation, erythroblasts and megakaryocytes were accompanied by capillaries [**A**]. The close proximity of those three cell types suggested their recent differentiation from common precursors (HSCs) at that location [**A**]. Also evident were forming vessels larger than capillaries, i.e. nucleated cells extending themselves around groups of erythrosomes before completing the enclosure [**B**]. The snail shaped cell in the upper left corner of [**B**] had asymmetrically distributed cytoplasm (a feature of a megakaryocyte) flattened against the abluminal surface of the forming vessel like a podosome, and nucleus partially divided by a radial sinus or invagination of nuclear membrane, suggestive of a potential for stretching. Cells closer to the erythrosomes also had such features. A cell undergoing mitosis is in the lower right corner of the image. Some cells, with ambivalent phenotype that had not specialized into either erythrosome or EC, made collagen in exuberant amounts, comparable to the size of their entire cytoplasm (instead of a few fibers like in Mouse 5) and the nucleus seemed to be converting into an erythrosome on its own [**C**]. However, because those proficient collagen makers were also perishing in the process of tissue building, the result was an area filled with scattered erythrosomes amidst massive amounts of collagen like in the left lower corner in [**D**]. Capillaries and larger vessels were seen side by side [**D**].

the diffusion range of metabolites. That event would be equivalent to the first heartbeat in a developing embryo.

Discussion

Cancer stem cells

Judging by the activities of cells evolving in our new experimentally created environment, we retrospectively assumed the presence of their precursors, in agreement with the functional TSCs definition. The question was which cells participated in the formation of the tumor vasculature and how did the vasculature form? At the outset, the components of the tumor niche (tumor spheroid, graft and local host tissues) did not have an ongoing vasculature formation. In both variants of the model, with and without homologous tissue graft, the new qualities emerged after the implantation (this report and the accompanying article[43], respectively). New tissues formed locally and integrated into the host animal. Some of the graft cells formed the new vasculature for the pseudo-orthotopically implanted tumor, whereas in the absence of the graft, some of the tumor cells eventually

evolved to do the same. In both types of the tumor niche (pseudo-orthotopic and ectopic) some local cells differentiated to form vasculature at the site of the tissue growth. Regardless of the origin (lineage) of those cells, one could think of them as SCs - based on the definition of such cells[37].

The amorphous continuously growing tumor mass was out of touch with tissue morphogenesis-controlling mechanisms but depended on the ability of the tumor cells to induce formation of vasculature either by CSCs or by local TSCs. Thus, tumors were subjected to selective pressure because those incapable of either inducing local nonmalignant SCs to form tumor-supporting vasculature or of generating their own vasculature[43] could not grow. The ability of the tumor to generate its own vasculature in the ectopic environment implied a conditional existence of CSCs, i.e. evident in one *in vivo* environment but not in the other (and not *in vitro*). Any single cell of the spheroid population could potentially establish new tumors in the orthotopic environment. However, large numbers of those cells would be necessary in a variety of ectopic environments, whether encountered by metastatic tumors or created experimentally[43]. One should not be surprised at finding HSCs markers among CSCs and ESCs because some of the features perceived in the literature as defining the stemness might be attributed to tissue growth, shared by malignant and non-malignant tissues. Our results showed that growing tissue sectors were capable of generating their own vasculature (blood and vessels) independently of the existing circulatory system and therefore recapitulated the embryonal vasculogenesis. However, the newly created blood-containing vascular segments did eventually fuse with the host vasculature whereas the embryonal vasculature does not fuse with the maternal one.

The vascular "sprouts" grew towards existing vessels, not away from them (Figure 11 & Figure S11 [A, C] and Figure 13 & Figure S13). Yet the new tumor-supporting vasculature observed here originated from the graft, not the tumor. To understand the paradox, one needs to keep in mind that the implanted components, tumor spheroid and graft, were related; both originated from the breast. When implanted separately, each behaved differently. The graft (injured lactating breast tissue) first produced new normal mammary epithelial ducts (results not shown) whereas the tumor initially used some of its own cells to feed the others, a fraction of which evolved into megakaryocytes and ECs[43]. However, when implanted together, breast tumor and breast tissue reconstituted the primary tumor in its native environment, as intended. Self-organizing potentials of the two influenced each other and a new dynamic balance emerged because of such interaction. At the same time, the host was responding to the injury inflicted by the surgical procedure associated with the implantation. That enabled the comparison of the tumor and the scar tissue vasculature formation side-by-side. The involvement of non-malignant TSCs in the formation of the tumor vasculature suggested that normal and malignant tissues share the cellular mechanism of vasculature formation. The developing nerves accompanying the forming vessels also indicated that those vessels were normal, yet they were as close to a muscle as to the tumor (Figure 11 & Figure S11). The growing undersupplied region likely initiated the process because without new substrates, the growth would be energetically prohibitive, regardless of the genetic makeup. The oxygen diffusion range and the maturity level of cells in the microenvironment shaped the initial vascular pattern. The presence of calmyrites in
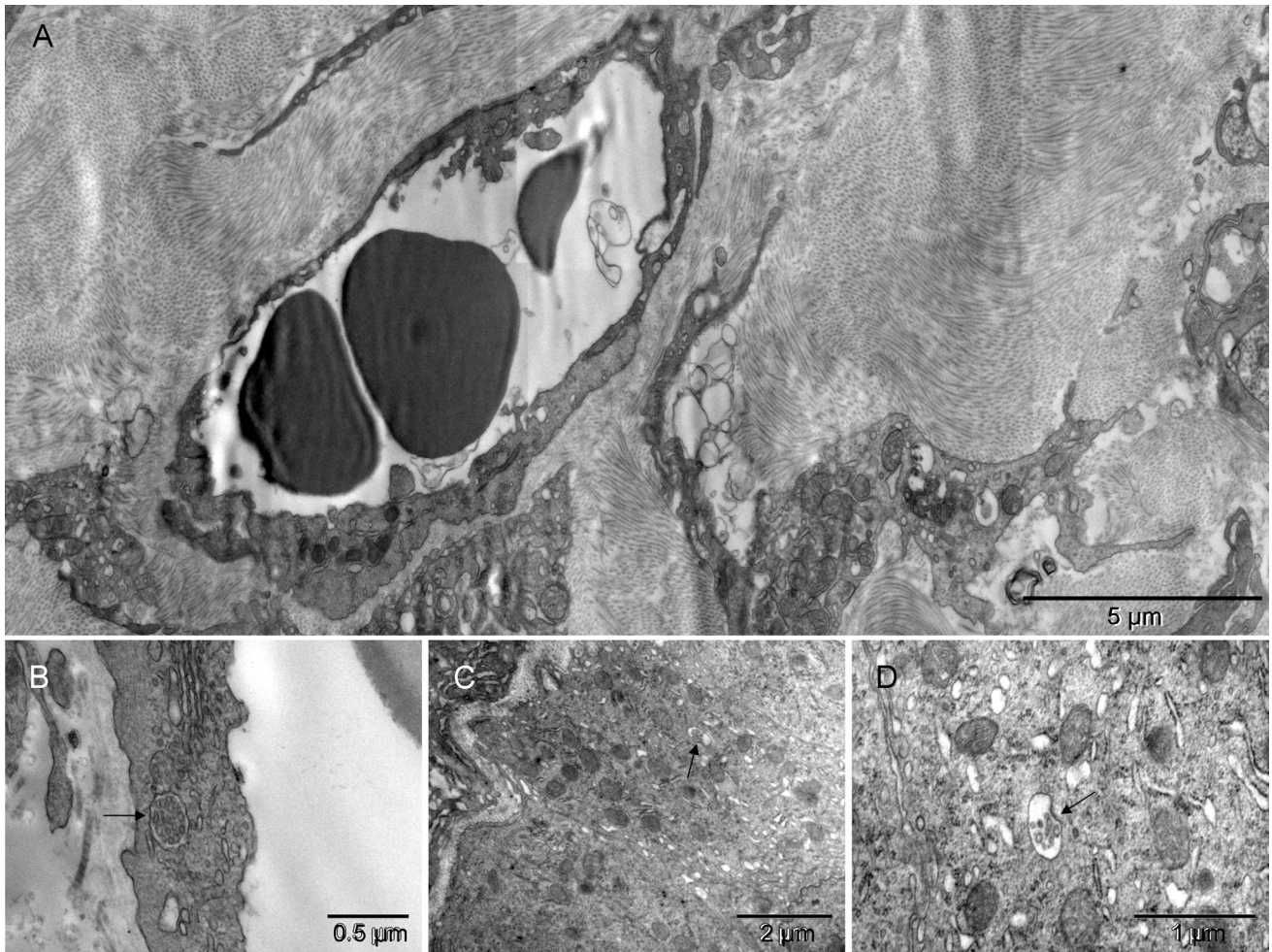
Figure 10. Role of collagen in morphogenesis of primitive vessels. The primitive vessels were embedded in copious amounts of collagen [**A**]. The wall of such vessels typically was polarized; it had caveolae on the luminal surface and collagen abluminally [**B**]. Collagen-making cell and tumor edges, accommodating each other's curvatures, revealed interaction between the two [**C**]. The tumor seemed to benefit from collagen support provided by the nonmalignant neighbor as well as appearing to have acquired the ability to synthesize some by itself. Arrows in [**B**, **C** & **D**] point towards intracellular bundles of collagen fibers; [**D**] is the enlarged collagen-containing region of [**C**]. Dilated cisternae of endoplasmic reticulum depleted of ribosomes to a variable degree resembled vesiculo-vacuolar organelles (VVOs)[59] [**D**].

non-malignant cells suggested that anaerobic metabolism was not unique for tumors either but could function in normal cells as an alternative, less-efficient pathway functional during mitosis and therefore more frequently used by tumors[43]. Morphologically, the tumor vascular pattern appeared abnormal because it never matured due to perpetual tumor growth[64]. Vascular tortuosity had been noticed to be a feature of young tissues[65,66], presumably in anticipation of growth. The blood flow would help to establish the hierarchical pattern for optimal functionality.

HSC lineages

Traditionally, the ontogenetic tree symbolizing cellular differentiation pathways, for instance hematopoiesis, consisted of arrows arranged in certain sequence and often branching but always pointing in the same direction, therefore signifying progress and irreversibility. Such a concept of phenotypic changes does not reflect great flexibility in

terms of the functions of differentiated cells for which compelling evidence has already been accumulated, including in vitro-induced pluripotent SCs[67,68], and is fast growing as the stem cell research prospers. The reliance of erythroblast and EC differentiation on natural selection, i.e. differentiation of HSCs by cytoevolution illustrated here for the first time, suggested "broken lines" for lineages (the dead ends and some stage skipping). The process was characterized by great variability of forms and perishing of nonfunctional ones that nevertheless must have contributed to the progress in differentiation of others by changing the microenvironment. The dead ends were demonstrated also in vitro[69]. Another interesting point related to cell lineages that emerged here as examples of the cell types thought of as mature that could trans-differentiate into other phenotypes. Megakaryocytes could become pericytes or ECs, depending on circumstances, and collagen-producers could become ECs. To trans-differentiate might be more practical than to
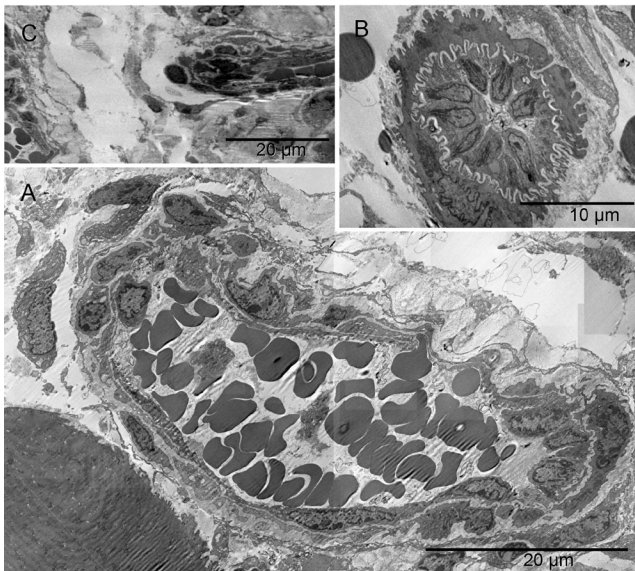
Figure 11. Morphogenesis of an artery (I). Forming lumen of the emerging vasculature fragment shown in [**A**] was occupied by free erythrosomes and platelets. That "vasculature piece" was not a vessel yet because it included blood elements that were being generated simultaneously with the vessel wall. The wall was incomplete at the time of image capturing. Structural differences along the circumference of the future lumen included a gap on the left side. Such lack of continuity and the irregular forms of erythrosomes also indicated that the forming vessel was not yet a part of the circulation. In that region, cells other than endothelial cells were recognizable, namely chromaffin cells and megakaryocytes at the outer side although their products (platelets) accompanied the erythrosomes in the lumen. The right side of the vessel wall was structurally the most advanced; it consisted of ECs uncharacteristically non-flattened. The shape of their nuclei and corrugation of the basement membrane between those cells and supporting pericyte suggested a potential for physical expansion. Such wavy basement membrane likely contained elastic fibers. The image in [**B**] could have been from a similar region cut in a perpendicular plane with regard to that in [**A**]; nuclei of the centrally located ECs had their radial sinuses oriented towards the basement membrane. That too could facilitate the expansion of the vessel. ECs in the middle part of the main image [**A**] were flattened; in the upper side one could see an erythrosome passing through. The spatial relationship between structures shown in [**A**] and in Figure 13 is demonstrated in [**C**].
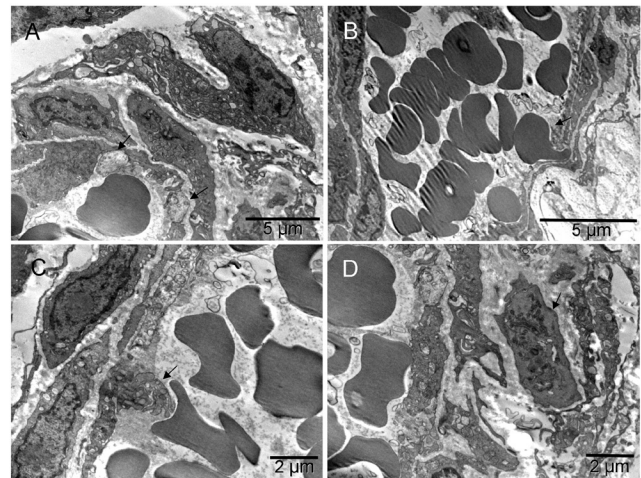

Figure 12. Ongoing structural rearrangements in the less advanced region of the forming artery (I). The images were from a section parallel to the one shown in Figure 11, i.e. from another region of the same vessel. Arrows point to two chromaffin cells in [**A**]; erythrosome, platelets and maturing platelets "*ante portem*", i.e. facing opening in the endothelium, are shown in [**B**,**C** & **D**], respectively.

Figure 13. Morphogenesis of an artery (II). A second forming complex vessel had a corrugated basement membrane at both ends of the elongated structure suggesting that the one in Figure 11 might not have been cut exactly parallel to its long axis. A round cell surrounded by a collagen-free region at the lower end suggested growth in that direction which happened to be pointing towards the first artery Figure 11 [**C**].

migrate long distances and deal with the forms that are no longer useful. The requirement for continuous regulation to maintain a differentiated phenotype was postulated previously[70]. A network of arrows pointing in different directions, including reverse, would represent the actual cellular differentiation pathways better than the traditional tree. "A good analogy likens cell types to metabolites in metabolic networks"[40].

Megakaryocytes are known to develop from bipotent erythroid/ megakaryocytic progenitor[7,53,71,72]. However, their morphogenetic role in establishing vascular pattern in the absence of ECs is new (Figure 1, Figure 2, Figure 11 & Figure S1, Figure S2, Figure S11). Addressing one of the unanswered questions in vascular biology[6,7] it demystifies the presence of platelets in the early embryo

and demonstrates that megakaryocytes and erythroblasts develop before ECs. Together they are capable of forming primitive vascular patterns without ECs. Given the chemical nature of CEA, (200 kDa glycoprotein containing about 50% carbohydrate) and its presence in tumors and in pregnancy, one could suspect that the presumed proteoglycans of ECM (Figure 1 & Figure S1) indeed
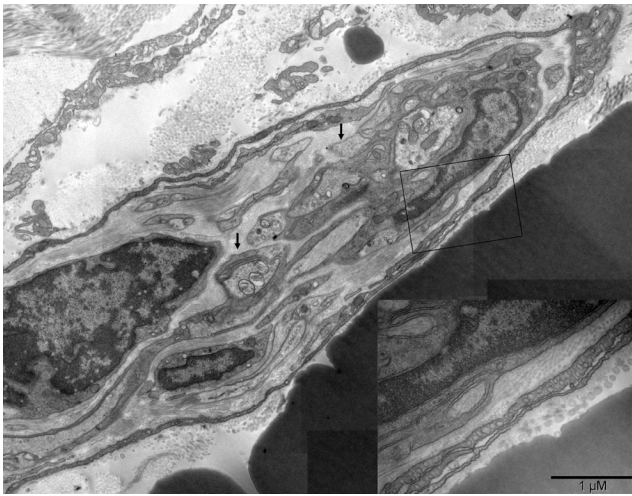
Figure 14. Developing peripheral nerve. Several nerve fibers were engulfed by Schwann cells on the right but progressing myelination could be recognized only on the one in the center with three mitochondria in the section plane (left arrow). Multiple nerve boutons with synaptic vesicles (right arrow) were present but mature synapses were absent. Surrounding the nerve fibers was one to three-layer neurothelium with abundant caveolae (insert in the right lower corner). Collagen fibers located internally were thinner (20–40 nm) than those lining the external surface of the neurothelium (60–100 nm). A giant erythroschizosome was located next to the forming nerve and it had similar dimensions (right lower corner behind the insert).

contain CEA[31]. The second dichotomy in the pathway corroborated the controversial derivation of ECs from hemangioblasts[73]. At a certain phase in vasculature morphogenesis, the three cell types co-localized as triplets and acted in concert. However, as the assembly of vessels progressed, megakaryocytes started positioning themselves abluminally suggesting their ability to trans-differentiate into pericytes (Figures 9 & Figure S9).

The presence of eosinophils (Figure 15 & Figure S15), neutrophils (Figures 1 & Figure S1), dendritic and plasma cells (not shown) in that environment, although relatively rare, suggests that they too differentiate locally and assist tumor growth. That possibility deserves further studies because, if confirmed, it would explain why the host immune system could tolerate the tumors. If primary tumors are similar enough to the tissue of origin to prompt local TSCs for vasculature formation, one could hardly rationalize the need for its rejection by the host. If, however, the tumor loses the tissue-specific characteristics, it would become alienated and dormant until an angiogenic switch occurred[43,74], which would not necessarily be immunogenic (e.g. medical implants are non-immunogenic). In further support of this theory, the lymphopoietic potential of mouse embryonic HSCs cells was indeed observed *in vitro* and *in vivo*[17,75].

Extramedullar erythrogenesis and tissue morphogenesis

The central role of the extramedullar erythrogenesis at every level of the dynamic complexity of vasculature formation was understandable because the ongoing tissue growth requires energy and nutrients. The complex issue of the origin and maturation of HSCs in developing embryos and their potential migration among
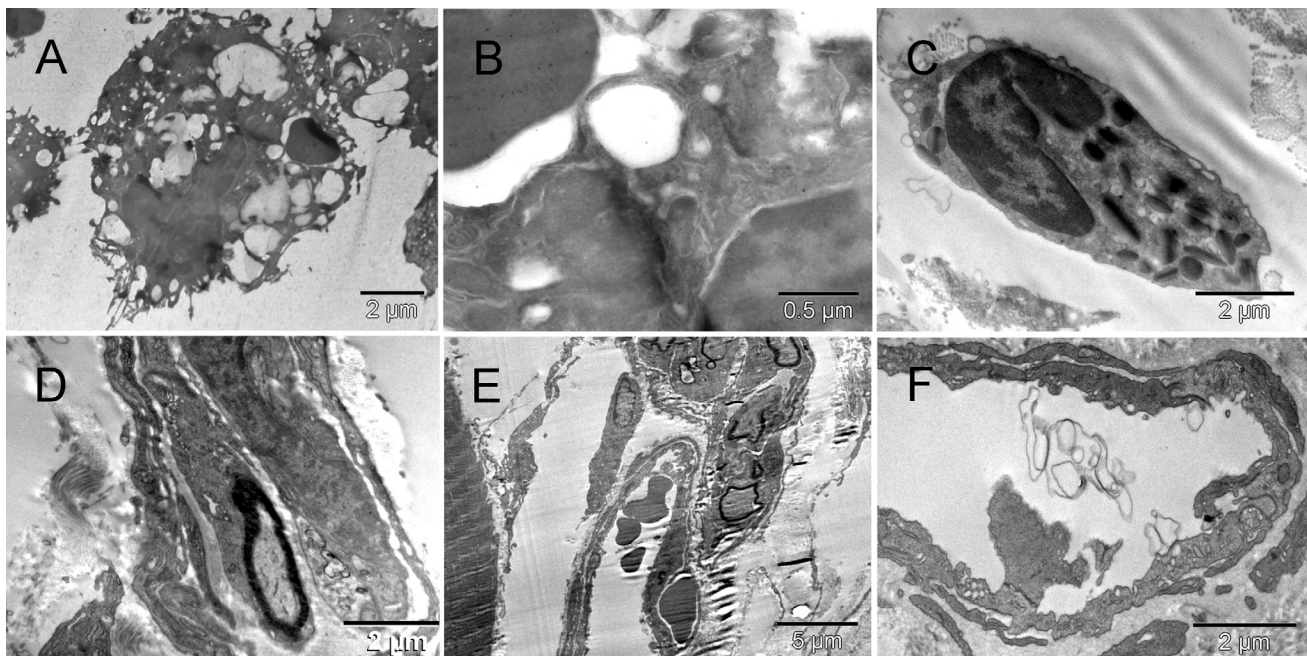

Figure 15. Rare findings. [**A** & **B**]: Erythrosome labeled with ubiquitin-detecting antibody, internalized by non-labeled macrophage (Mouse 5). [**C**]: Eosinophil (Mouse 3). [**D**]: Myelinated nerve fiber engulfed by Schwann cell (Mouse 2). [**E**]: Forming vessel located between muscle and nerves (Mouse 2). [**F**]: Empty vein or lymphatic vessel with an internal valve (Mouse 2).

AGM, yolk sac, umbilical artery, vitellin artery, placenta and fetal liver[76] was echoed in the model used here. Without the guidance from the mature bone marrow niche, the erythrogenesis was recapitulating the embryonal stages. Calmyrites contributed a new criterion for grading the maturity level of erythropoiesis.

Our observations offered new understanding of vasculature morphogenesis in relation to tissue morphogenesis. For example, plasticity of cells became well recognized but often perceived as "puzzling, surprising, intriguing, provoking", etc. as single TSC types or even clones gave rise to multiple phenotypes unexpectedly. Epithelium evolved from bone marrow progenitors[77], hematopoietic cells from endothelial or neuronal cells[75,78,79], blood from brain[80] or muscle[81,82], muscle from HSCs[82,83], and HSCs from stromal-vascular fraction of adipose tissue[21,84], causing the confusion. The common presence of the hematopoietic component in those heterogeneous differentiated populations derived from TSCs was striking. It suggests that progenitor cells committed to a specific tissue type also have hematoblastic potential. One can anticipate more reports on finding erythropoietic cells during procedures intended to isolate tissue-specific cells. That reasoning does not contradict trans-differentiation of cell types other than those involved in erythropoiesis. For example, neuronal cells were shown to change their phenotype to endothelial cells when co-cultured with (ECs)[85]. Historically, the HSC lineage has shaped the traditional belief in terminal differentiation but, as discussed below, that lineage turned out to be a special case rather than the archetype from which to extrapolate to other tissues. Yet supposedly all connective tissues (and possibly others) derive from HSCs and therefore, transplantation of HSCs rather than mesenchymal SCs would be the choice therapy for genetic deficiencies of connective tissues, making HSCs a panacea for multiple related illnesses[86]. However, our results suggest the opposite. All tissues, at all stages of life, might have hemato-lympho-vaso-neuro-adipo-poietic potentials as long as they have the potential to grow or to repair themselves. However, execution of that potential would depend on morphogenesis-controlling factors and the availability of proper substrates. Various types of hematopoiesis (primitive, definitive and subclasses of those) reflect the differentiation levels of the tissues harboring the process. In an emergency, even endothelium could become hemogenic[87].

Understanding the mechanisms regulating tissue morphogenesis could have therapeutic implications. For example, the observation that collagen is essential for the process could be useful. Assuming that ECM of tumor tissue might be unprotected with tissue inhibitors of metalloproteinases (TIMPs), as was shown to be the case in embryo[88], one could envision pharmacological intervention with proteolytic enzymes.

The organoblasts concept
The classic functional definition of the adult TSCs was amended in 2002 to include its flexible and regulated tissue self-organization capability based on cell-cell and cell-environment interactions[37]. The amended definition allowed for the assumption that TSCs have tissue specificity and the ability to form vasculature *de novo* when needed. Conceptually one could view TSCs as histo-hematoblasts, as we did initially. Just like TSCs and SCs in general, the histo-hematoblasts was a concept, not a clone[37]. Which cells would

produce a new piece of tissue or its vasculature did not have to be predetermined during embryogenesis but later, when and where the growth was to take place. The location of tissue growth must be governed by organogenesis-controlling factors like BMP4[89–91]. An example demonstrating the spatial correlation between hematopoiesis and regions of tissue growth is available for the mouse embryo[92]. Simply put, when traced back along their ontogenetic lineage, cells engaged in building new vasculature for the growing part of a tissue would not all turn out to belong to a single HSC clone. Such multi-origin does not imply their universal applicability as transplants; as mentioned above, the developmental compatibility was shown to matter to some extent[18]. Another practical aspect that follows is that a strategy to stop the vasculature formation in tumors should not target specific precursor cells but rather the process itself, regardless of the lineage of cells executing the tumor supporting function. To think of SCs as "some cells" might be helpful. Due to the self-organizing potential of tissues in higher organisms, at any phase of growth and development or life of an individual, some cells in the growing region of an organ might be capable of addressing the basic metabolic needs locally, and of establishing communication with the rest of the organism. Which cells of a given organ they are, may be neither predetermined nor critical but dictated by morphogenesis-regulating factors (malfunctioning in tumors) and local energy metabolism requirements (applicable to tumors).

The concept of histo-hematoblasts was rooted in the fundamental role of neo-hematopoiesis in tissue morphogenesis, namely, fueling metabolism of any tissue mass exceeding diffusion range of oxygen (100–200 µm[93,94]; 150 µm[64]) and presumably of nutrients. Neo-hematopoiesis appeared to be the core of the process, both figuratively speaking and literally. Emerging erythrosomes, known for their ability to secrete ATP[58], formed the central point to which other cells were chemotactically attracted and around which endothelium evolved eventually with ATP-ase located in caveolae[60–63]. What triggered the local (extramedullar) vasculature formation was the localized incremental tissue growth. Any tissue growth, (developmental, repair-related or malignant) would require new vasculature; whereas, proliferation of cells replacing those that perish while fulfilling their physiological functions would not. Examples are intestinal and skin epithelia, hair follicles and secretory cells of some glands (as discussed in[87]). One could think of TSCs as "kits" containing potentials for all necessary elements of the tissue to be built. Chromaffin cells participated in assembling the new artery (Figure 11, Figure S11 & Figure 12, Figure S12) and cells from the immune system were present in that environment too. Developing nerves paralleled the forming vessels of similar dimensions (Figure 15, Figure S15 [E] and Figure 4 in[43]). GATA-2 transcription factor required for hematopoiesis was also reported to be involved in the maintenance of the pool of ventral neuronal progenitors[92]. Moreover, existence of common neural and vascular patterning tools (signaling molecules like ephrins, netrins, slits, semaphorins and neuropilins) was in fact pointed out earlier[95,96]. The correlation of vasculature formation with the local development of nerves, mentioned above and elsewhere[97–101], called for modifying the concept of histo-hematoblasts to the organoblasts concept, to cover the observed phenomena more adequately.

The organoblasts (Organo-Bs) is designed to be a generic term for such organ-committed precursor cells. The plural of the term is

deliberate here, like in the case of SCs, because those cells neither belong to a unique lineage nor are committed to a specific tissue type within an organ. In particular cases they would be for example: Nephro-Bs (kidneys), Hepato-Bs (liver), Osteo-Bs (bone), Dermo-Bs (skin), Pulmo-Bs (lungs), Entero-Bs (gut), Sarco-Bs (muscle), Spleno-Bs (spleen), Thymo-Bs (thymus), Ovario-Bs (ovary), Testo-Bs or Orchio-Bs (testes), Cerebro-Bs (brain) and Cardio-Bs (heart) and so on. Hemangio-Bs and Neuro-Bs would derive from the organoblasts of each organ independently to form vasculature, lymphatics and peripheral nerves. Accordingly, in the formation of any new tissue (or in the growing segment of an existing tissue), some of the growing cells would become hematoblasts or neuroblasts to connect them to the rest of the given organ in the system. Naturally, such a mechanism of vasculature morphogenesis would result in organ-specific variability in the endothelium. That would be consistent with published reports on the presence of tissue-specific markers on endothelium in particular organs, i.e. functional variability of endothelium in different organs[102–107] as well as ultrastructural differences. Brain vessels provided the most prominent example[108]. The current definition of TSCs implies their potential to provide differentiated cells specific for a given tissue. The difference between TSCs and organoblasts (or organ SCs) is the ability of the latter to give rise to cells of specific tissue parenchyma as well as all the accessory cells necessary to maintain system homeostasis. All those cells would be locally differentiating from the organoblasts at the site of incremental tissue growth.

From the evolutionary perspective, flexibility is more valuable than rigid perfection of the complex systems. Phylogenetic analysis applied to mouse cell lineages have indicated that extensive cellular mixing homogenized the lineages in the embryo before gastrulation[41]. Therefore, up to that stage of development, the cells were functionally equivalent. Consequently, dissimilar lineages participated in morphogenesis of particular tissues during organogenesis. Such redundancy combined with cell plasticity and the natural selection at the cellular level might have been compensating for the high number of mutations happening at every mitosis. *C. elegans* can afford to lose an entire individual because one organism can produce ~1000 fertilized eggs, whereas mammals are too complex to take care of mutations that way[41].

Tissue definition

The tissue definition based on the organoblasts concept would consist of two parts: (1) organ location (liver, heart, brain, stomach, pancreas, bone, striated muscle, ovary etc.), and (2) specific function, either unique for that organ, or system integrating (nerves, vasculature and lymphatics), or providing structural integrity. Tissues related to the latter two functions could be similar in different organs but not identical, as known for the endothelial surfaces. [Examples: brain grey matter, brain white matter, brain meninges, brain vessel; gut epithelium, gut smooth muscle, gut vessel; heart artery, heart vein, heart muscle; liver parenchyma, liver vessel; lung epithelium, lung endothelium, lung pulmonary pleura, lung costal pleura; lymph node capsule, lymph node nodule, lymph node hilum; peripheral nerve dendrites, peripheral nerve Schwan cells, peripheral nerve neurothelium; auricular cartilage, bronchial cartilage, articular cartilage, growth plate cartilage; bone marrow, bone cancellous, bone trabecular, bone periosteum, bone capillary; tumor parenchyma, tumor vessel, etc.]. There is more to organ development than differentiation of specific cell types. Dramatic qualitative changes of the tissue fabric in growing organisms occur by tissue remodeling; for example, bone morphogenesis involves formation of properly shaped cartilage first and its subsequent replacement with calcified tissue. In our model, free erythrosomes scattered in abundant collagen formed a scaffold that could support morphogenesis of the malignant tissue or scar.

The position of vasculature as a specific type of connective tissue equal in rank to other differentiated tissues, i.e. created during embryogenesis, deserves to be reassessed. Our results suggest extending the acceptance of the multiple origins of HSC precursors in the embryo to any tissue growth (malignant or reconstructive), also after birth. The vasculature formation (blood and vessels) is unique because it must be a part of any tissue growth, whether developmental, pathological or reconstructive and regardless of age, not just during embryogenesis. The novelty here was that not only vessels but also blood formed *de novo* at the location of growing tissue, not just in bone marrow and spleen. That could presumably occur in any organ. Under stress, a fraction of any tissue could feed the rest of the population if that meant survival of some cells. How the conversion of living cells into a meal could happen would depend on what kind of cells they were and on the microenvironment. Hematopoiesis appeared to have fundamental but accessory role in all tissues. That is why following HSC lineage was not a trivial issue. The implications go beyond cell lineages; they extend to organogenesis.
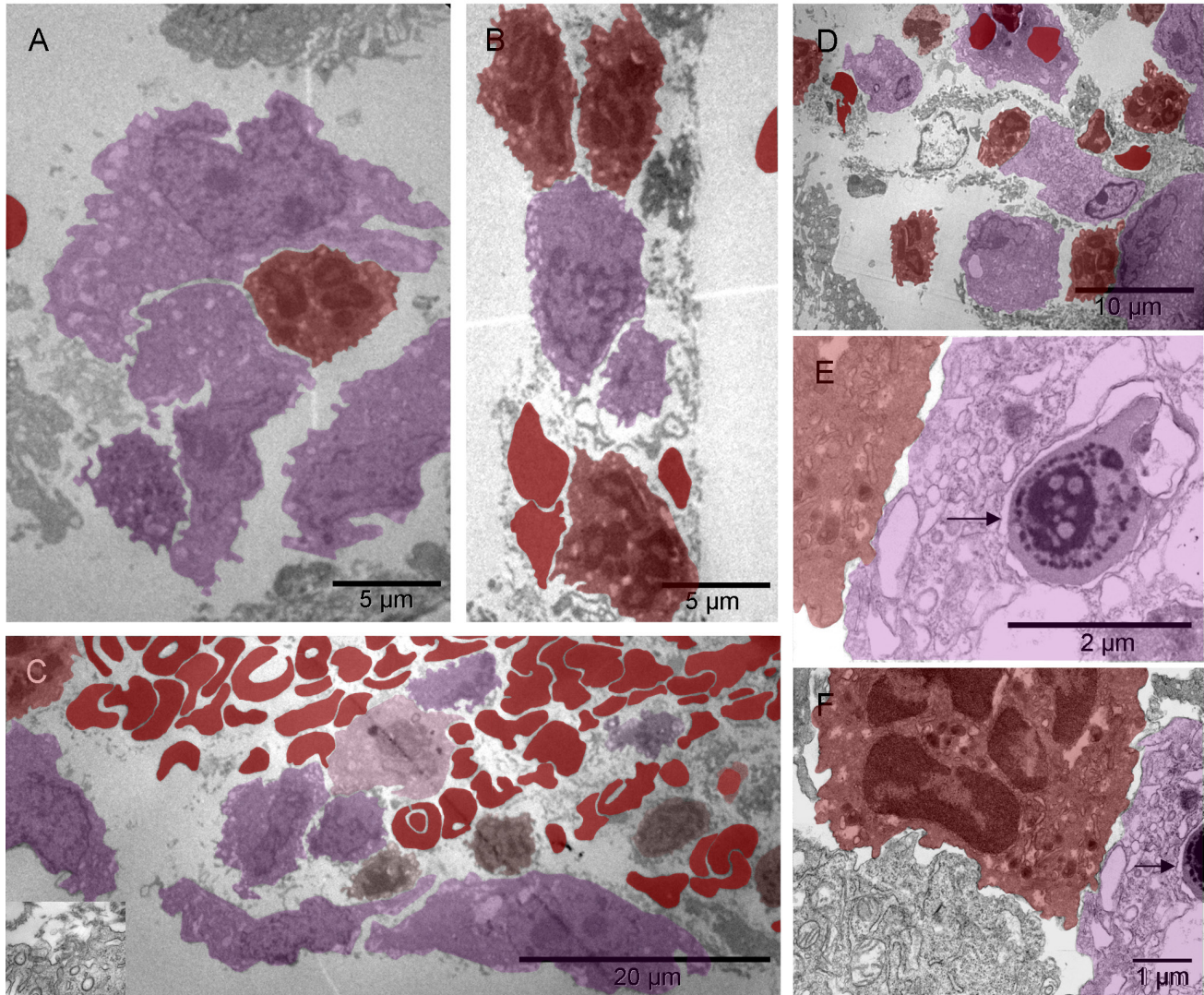
Supplementary material

Figure S1. A blueprint for vascular pattern created by migrating erythroblasts and megakaryocytes. The pattern-forming heterogeneous population of the cells migrating in the hyaline membrane consisted of (a) those with large nuclei occasionally containing double nucleoli and with asymmetrically distributed, irregularly shaped, large cytoplasm and satellite platelets i.e., megakaryocytes (purple), and (b) those with atypical, lobular, heterogeneously dark nuclei and dark cytoplasmic granules in the absence of mitochondria, usually accompanied by erythrosomes (red), i.e. most likely erythroblasts (light red) [**A**]. The four elements, cellular and sub-cellular (erythrosomes and platelets), appeared evenly dispersed among each other like in the narrow (about capillary short dimension) column in [**B**] or the megakaryocytes that displayed a tendency to migrate to the periphery of the larger cluster and surround the other elements [**C**]. Those poorly differentiated cells were probably bipotent, megakaryocyte and erythroid, progenitors (brown) [**C**]; compare with Figure 8 in[55]. The cellular and sub-cellular elements appeared to be held together with extracellular fibrous components, possibly proteoglycans and little collagen (the insert in [**C**]). The resulting red pattern appeared as a vascular network under low magnification of dissecting microscope. The parallel arrangement of extracellular, short, non-collagen fibers suggested mobility for the cells secreting them [**D**]. The extra-cellular matrix (ECM) producer [**E**] located to the right of the erythroblast [**F**] contained a composite dense body (arrows in [**E** & **F**]) characteristic of platelets (see Figure 111-1, E in[56]).
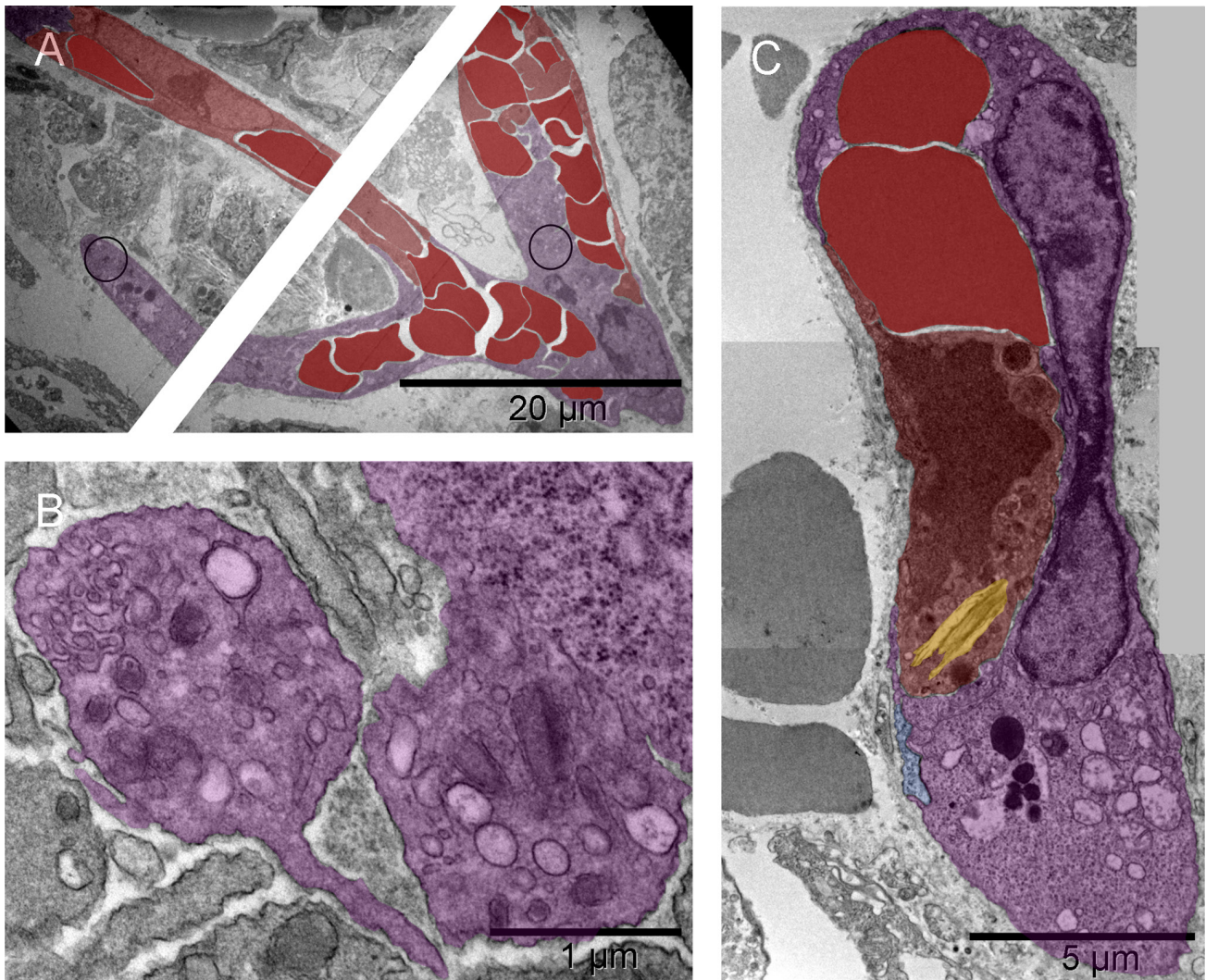
Figure S2. Primitive vascular pattern formed by megakaryocytes without endothelium. Primitive vascular pattern in the tumor-harboring solid tissue below the hyaline membrane consisted of megakaryocytes and platelets (purple) engaged in direct and tight contact with one another and with erythrosomes and erythroblasts (red). There were no ECM-filled spaces left between them nor was there an additional cellular layer covering those elements. The elongated branching structure in [**A**] appeared kept together by megakaryocytes and platelets (N.B. the cutting imperfection mentioned in Figure 2 has been removed here). In the two circled regions of that structure, incomplete separation of platelets from megakaryocytes provided ultrastructural evidence for their identity and for an ongoing process of generating platelets at that location. One region was the bifurcation area at the base of the right almost vertical branch, enlarged in [**B**] and the other was the tip of the lower left branch (enlargement not shown). Evidently, megakaryocytes were capable of organizing erythrosomes into branching primitive vascular structure before ECs emerged to provide protective walls of a vessel. In a smaller elongated structure of similar nature, although without platelets in the section plane, one of the cells contained an Auer body [**C**], previously described in neutrophils from cases of leukemia and defined as azurophilic, large, elongated granules (Figure 64-10 in[57]). The upper part of that cell contained two erythrosomes; whereas what remained of the nucleus had a different texture compared with that of the nucleus in the second cell of that complex. The prominent dark granules of the latter resembled those in the cell next to the megakaryocyte from the tip of the lower branching structure in [**A**]. If the irregularly shaped seemingly empty space next to those granules was a prototype of a lumen then both those cells could have potentially been angioblasts.
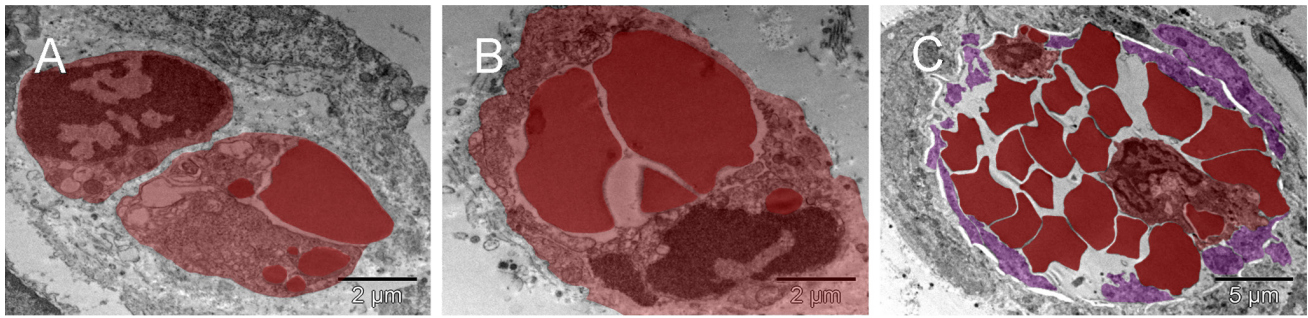
Figure S3. Extramedullar erythropoiesis via nucleo-cytoplasmic conversion. The single cells undergoing structural remodeling in the nucleus and cytoplasm represented at slightly different stages of erythropoiesis [**A** & **B**]. Conceivably, a few such cells (red), when gathered into a cluster, could fill up a larger space with erythrosomes creating a cobble stone pattern, also called 'erythropoietic lake' or myeloplaxes [**C**]. Platelets and megakaryocyte (purple) were recognizable at the periphery of the cluster.
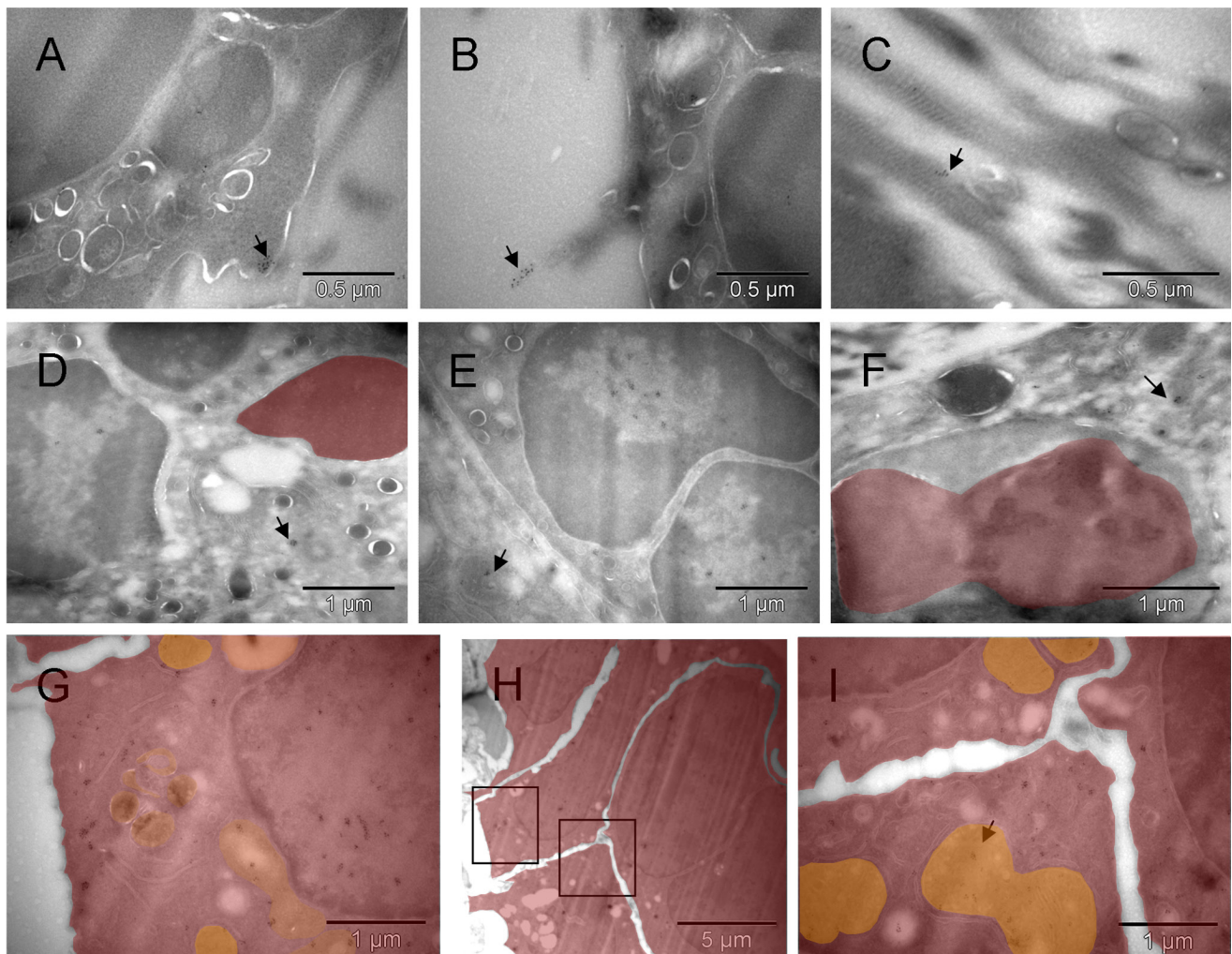

Figure S4. HSCs and their progenitors at the tumor site labeled with CD34 marker. Clusters of the gold label were found on the cell surface, in the nucleus, cytoplasm and mitochondria of cells morphologically fitting the description of erythroblasts [**A**, **B**, **D** & **E**] and on extracellular collagen fibers produced by them [**B** & **C**]. A fragment of cell with mixed phenotype is shown in [**F**]. The cluster of CD34-labeled giant erythroblasts (red), potentially leading to myeloplaxes, contained one cell with a double nucleus (right side in [**H**]). Two regions of [**H**] are enlarged in [**G** & **I**], left and right respectively, to show oversized mitochondria (orange), some converting into peroxisomes (dark & orange) [**G**]. That cluster of cells was bigger than the one shown earlier (Figure S3C), and the presence of mitochondria despite clear commitment to erythropoiesis suggested that here the process was more efficient. Arrows point out some clusters of Au grains.
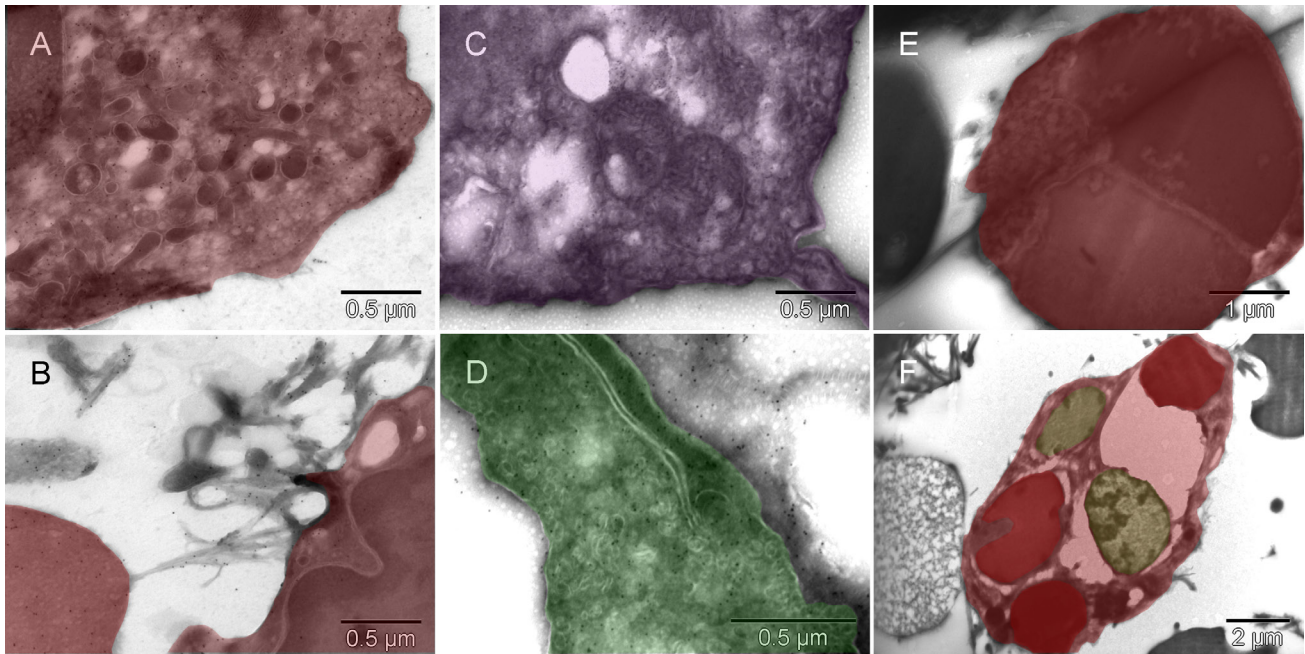
Figure S5. Cells of graft origin labeled with GFP under ubiquitin promoter. GFP-specific label was present in erythroblasts (red) [**A**], primitive erythrosomes (red) like the one separating from the cell that made it (left lower corner in [**B**]), platelets (purple) [**C**] and in EC (green) [**D**]. Morphologically interesting cells, erythroblast [**E**] and perishing hemangioblast [**F**] stained with nonspecific antibody are shown at low magnification (they had no gold grains). The erythroblast was entirely consumed by a successful incremental conversion into at least three erythrogenic vesicles (red) [**E**] and the cell with ambivalent phenotype [**F**], possibly hemangioblast, contained three internal vesicles resembling erythrosomes (red) and two of comparable size that appeared to be failing as erythrosomes (green) (partially electron lucent ones).
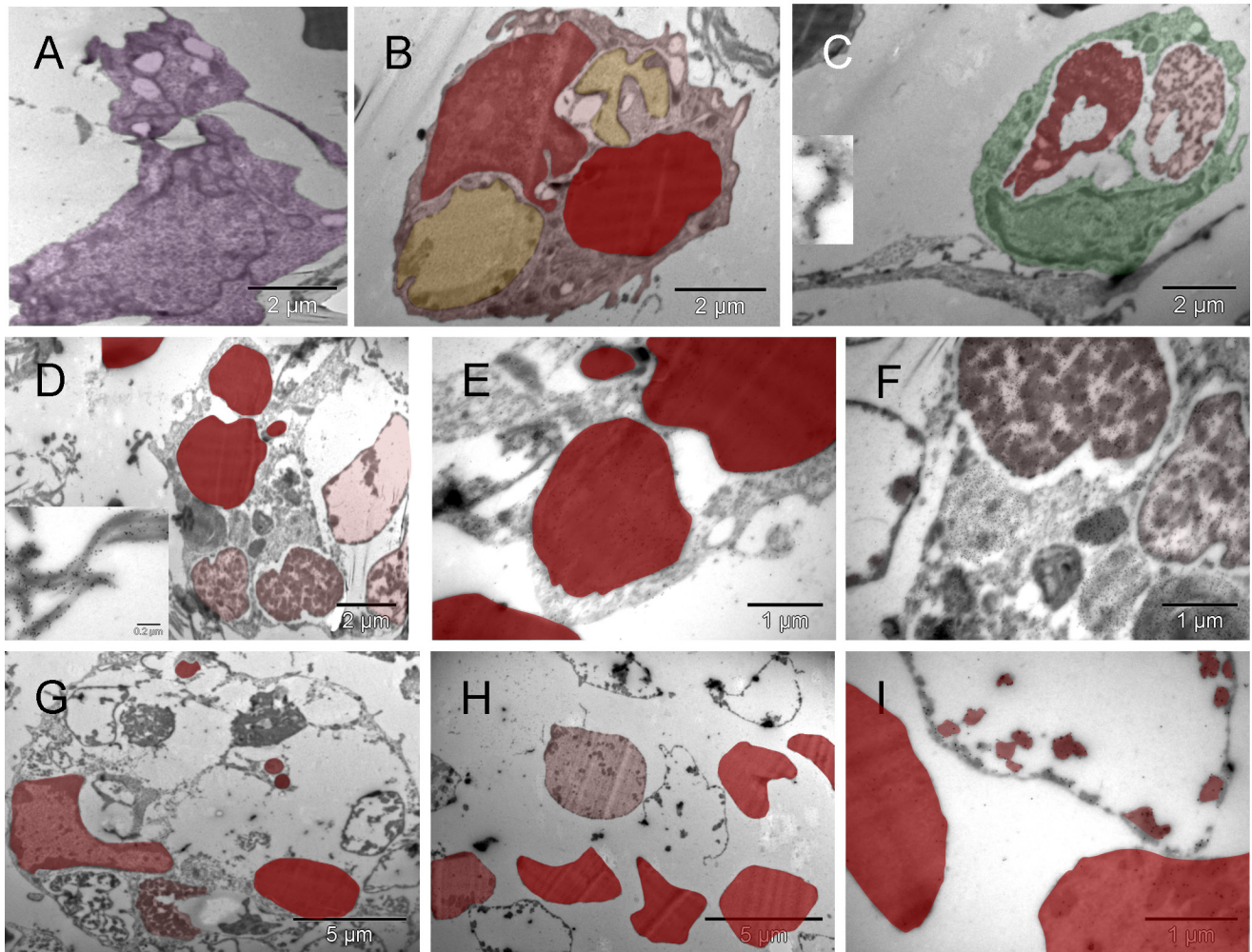
Figure S6. HSCs differentiation by evolution. The cells shown in the upper row [**A**, **B** & **C**] were located in the hyaline membrane 5 μm (or less) apart from one another (Figure S14b) suggesting their relatively recent derivation from a common precursor. The first, irregularly shaped cell with platelet-resembling attachment was probably a megakaryocyte (purple) [**A**]. The second one (mixed shades of red), had four large vesicles but only one of them was similar in size and electron density to a cell-free erythrosome (right upper corner in [**A**]), whereas two other vesicles (yellow) were much lighter with the exception of small patches at the periphery, and the fourth one was probably an incompletely converted nucleus [**B**]. The third cell (green) had two large vesicles (red and pink) and both appeared to represent different stages of degradation of the material they were made of [**C**]. The outer membrane of that cell was at one side connected to another cell via calmyrin-containing extracellular fibers (insert in [**C**]). Both cells with the large vesicles made impression of cells with mixed phenotypes with some inclinations to specialize in either producing erythrosomes [**B**] or forming a lumen [**C**]. Fields shown in [**D**–**I**] were in the same section; they represented what seemed to be left after internal remodeling of polyploidal cells or multi-cellular clusters [**D** & **G**]. There were cell-free erythrosomes as well as empty vesicles, some broken [**H**]. Clearly, cells were perishing because of such restructuring but they were also changing the microenvironment. Insert in [**D**] shows calmyrin-specific label on fibers of ECM. [**E**, **F** & **I**] are enlarged regions from [**D**] and [**H**], respectively.
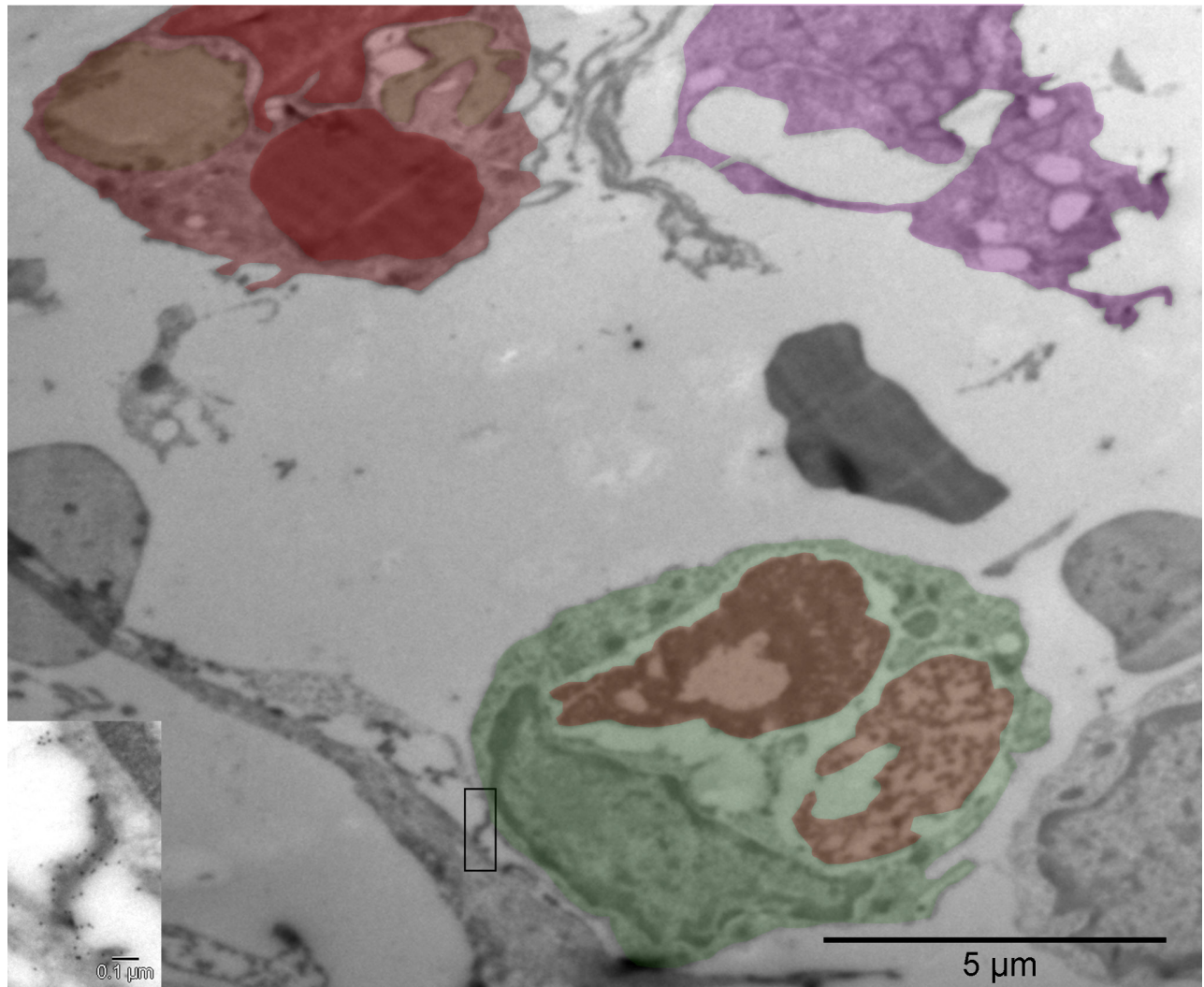
Figure S7. **Relative location of megakaryocyte (purple), erythroblast (red) and ECs (green) precursors *in situ*.** Compare with Figure S4 [A, B & C]. The insert shows calmyrin-containing extracellular fibers connecting the adjacent cells.
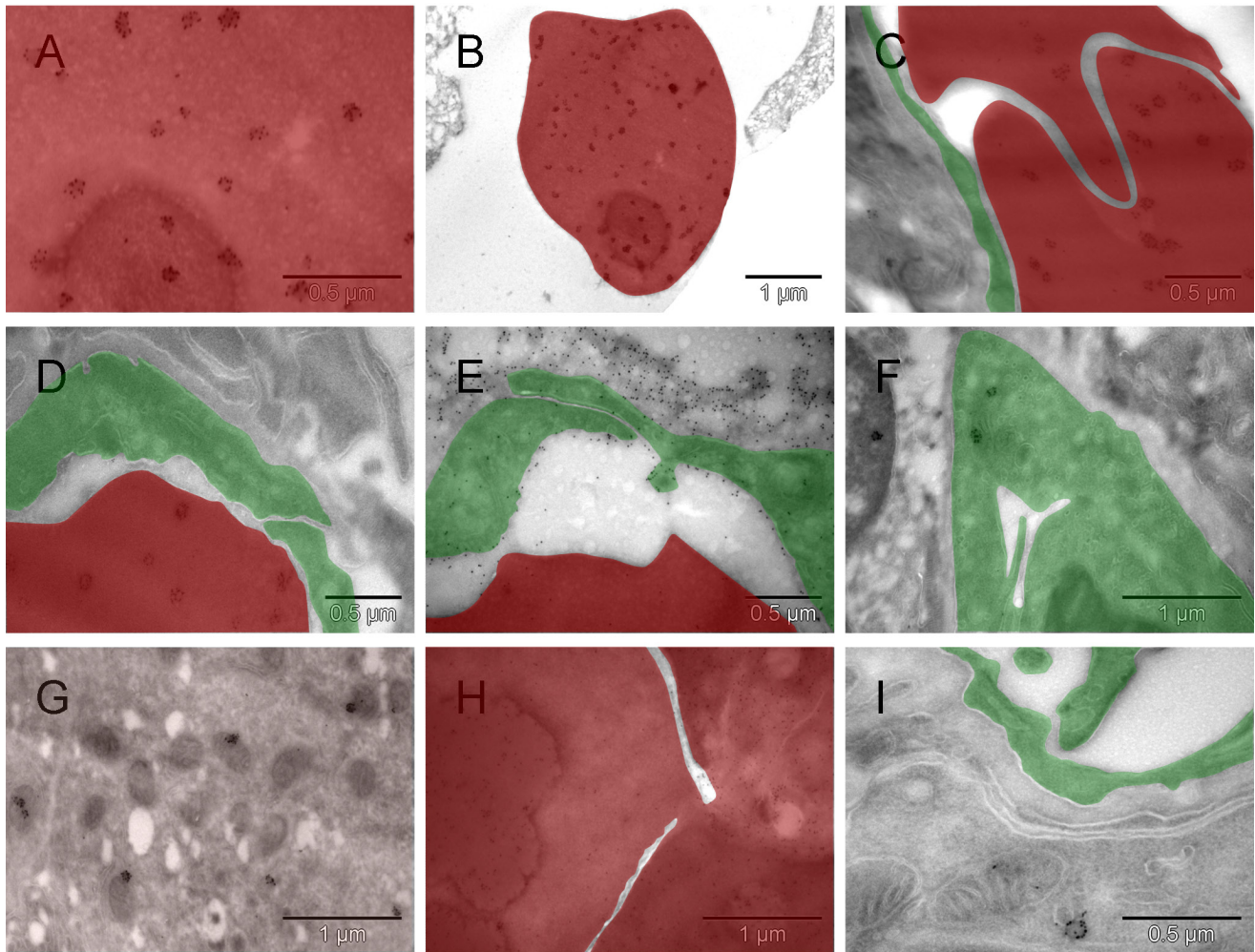
Figure S8. Calmyrite: a new ultrastructural entity involved in anaerobic metabolism. Uneven distribution of the abundant calmyrin-specific label in erythrosomes (red) from the solid tissue under the hyaline membrane was striking [**A**, **B**, **C** & **D**]. No such clusters were seen extracellularly [**E**]. The gold particles appeared arranged with certain symmetry in clusters of about 6 to 12, as if the protein became a part of distinct para-crystalline ultrastructures that in less differentiated regions were not formed ([**E**] and Figure S4). Such gold grain clusters were also present in ECs (green) [**F**] and tumor cells (brown) [**G**] where small dark mitochondria suggested hypoxic distress. In a giant cell, the uneven distribution of scattered calmyrin-specific label and heterogeneity of electron density indicated an ongoing process of erythrogenic conversion [**H**]. One calmyrite in a section from normal rat lung is shown in [**I**]. Those ultrastructural para-crystalline elements visualized by calmyrin-specific label are being described here for the first time and referred to as calmyrites.
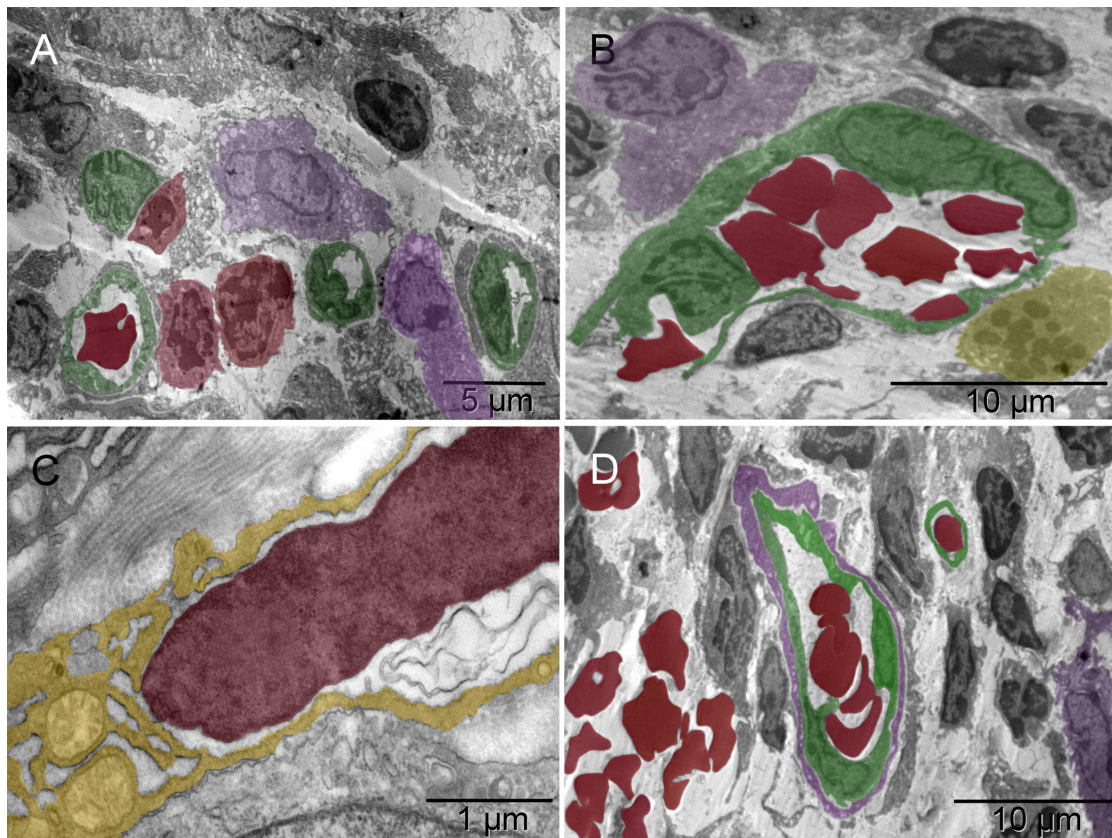
Figure S9. Progress in cellular differentiation and assembly of new vessels. Three weeks after implantation, erythroblasts (red) and megakaryocytes (purple) were accompanied by capillaries (green) [**A**]. The close proximity of those three cell types suggested their recent differentiation from common precursors (HSCs) at that location [**A**]. Also evident were forming vessels larger than capillaries, i.e. nucleated cells extending themselves around groups of erythrosomes before completing the enclosure (green) [**B**]. The snail shaped cell (purple) in the upper left corner of [**B**] had asymmetrically distributed cytoplasm (a feature of a megakaryocyte) flattened against the abluminal surface of the forming vessel like a podosome, and nucleus partially divided by a radial sinus or invagination of nuclear membrane, suggestive of a potential for stretching. Cells closer to the erythrosomes also had such features. A cell undergoing mitosis (bright yellow) is in the lower right corner of the image. Some cells, with ambivalent phenotype that had not specialized into either erythrosome or EC, made collagen in exuberant amounts, comparable to the size of their entire cytoplasm (yellow) instead of a few fibers like in Mouse 5, and the nucleus (red) seemed to be converting into an erythrosome on its own [**C**]. However, because those proficient collagen makers were also perishing in the process of tissue building, the result was an area filled with scattered erythrosomes amidst massive amounts of collagen like in the left lower corner in [**D**]. Capillaries and larger vessels were seen side by side [**D**].
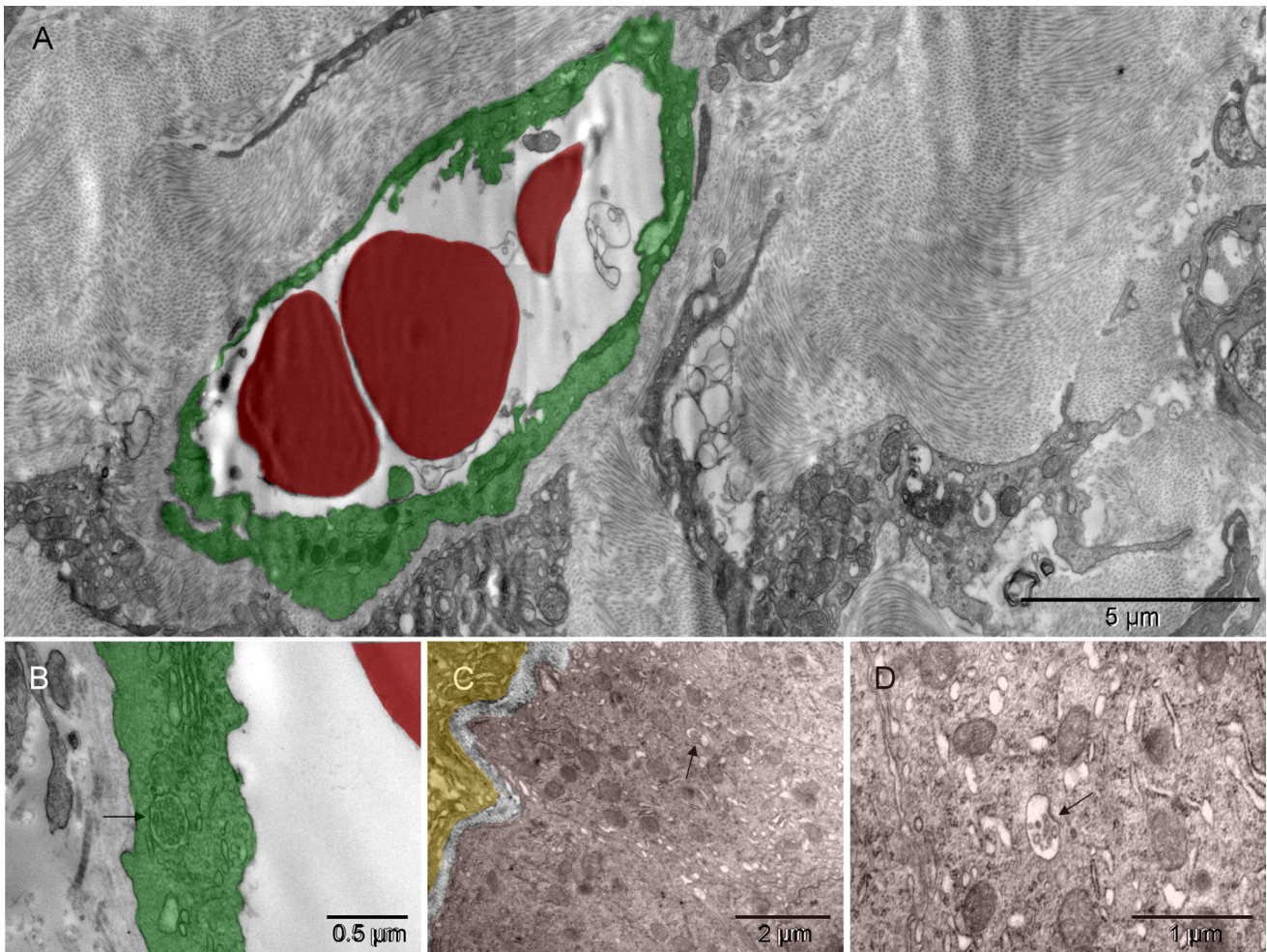
Figure S10. Role of collagen in morphogenesis of primitive vessels. The primitive vessels were embedded in copious amounts of collagen [**A**]. The wall of such vessels (green) typically was polarized; it had caveolae on the luminal surface and collagen abluminally [**B**]. Collagen-making cell (yellow) and tumor edges (brown), accommodating each other's curvatures, revealed interaction between the two [**C**]. The tumor seemed to benefit from collagen support provided by the nonmalignant neighbor as well as appearing to have acquired the ability to synthesize some by itself. Arrows in [**B**, **C** & **D**] point towards intracellular bundles of collagen fibers; [**D**] is the enlarged collagen-containing region of [**C**]. Dilated cisternae of endoplasmic reticulum depleted of ribosomes to a variable degree resembled vesiculo-vacuolar organelles (VVOs)[59] [**D**].

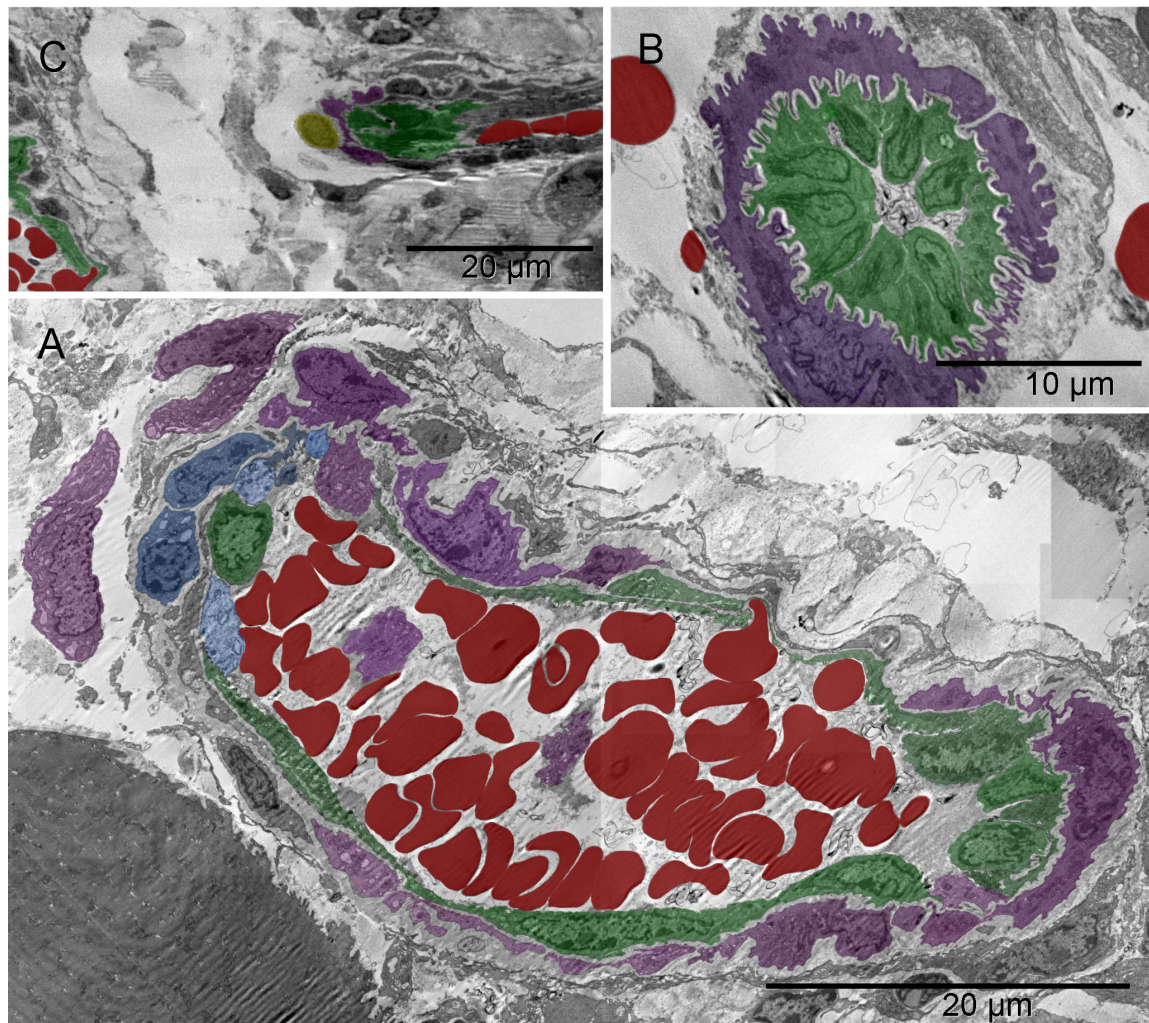**Figure S11. Morphogenesis of an artery (I).** Forming lumen of the emerging vasculature fragment shown in [**A**] was occupied by free erythrosomes (red) and platelets (purple). That "vasculature piece" was not a vessel yet because it included blood elements that were being generated simultaneously with the vessel wall. The wall was incomplete at the time of image capturing. Structural differences along the circumference of the future lumen included a gap on the left side. Such lack of continuity and the irregular forms of erythrosomes also indicated that the forming vessel was not yet a part of the circulation. In that region, cells other than endothelial cells were recognizable, namely nerve and chromaffin cells (dark and light blue, respectively) and megakaryocytes (purple) at the outer side; although their products, platelets (purple), accompanied the erythrosomes in the lumen. The right side of the vessel wall was structurally the most advanced; it consisted of ECs (green) uncharacteristically non-flattened. The shape of their nuclei and corrugation of the basement membrane between those cells and supporting pericyte suggested a potential for physical expansion. Such wavy basement membrane likely contained elastic fibers. The image in [**B**] could have been from a similar region cut in a perpendicular plane with regard to that in [**A**]; nuclei of the centrally located ECs had their radial sinuses oriented towards the basement membrane. That too could facilitate the expansion of the vessel. ECs in the middle part of the main image [**A**] were flattened; in the upper side one could see an erythrosome passing through. The spatial relationship between the structures shown in [**A**] and in Figure S10 is demonstrated in [**C**].
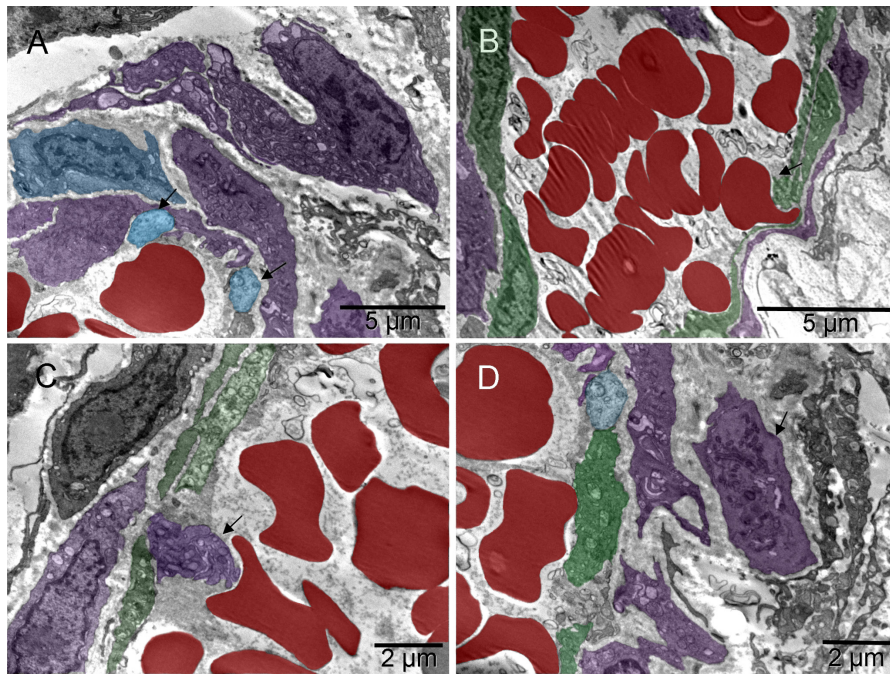
Figure S12. Ongoing structural rearrangements in the less advanced region of the forming artery (I). The images were from a section parallel to the one shown in Figure S8, i.e., from another region of the same vessel. Arrows point to two chromaffin cells (blue) in [**A**]; erythrosome (red), platelets (purple) and maturing platelets "ante portem" i.e. facing the opening in the endothelium (green), are shown in [**B, C** & **D**], respectively.
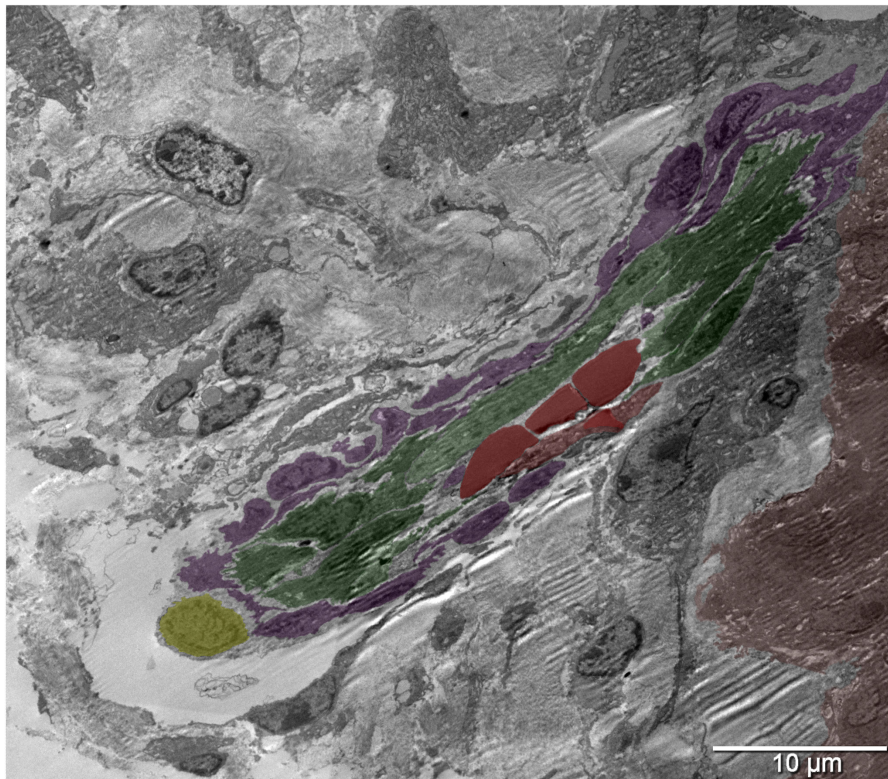
Figure S13. Morphogenesis of an artery (II). A second forming complex vessel had a corrugated basement membrane at both ends of the elongated structure suggesting that the one in Figure S8 might have been cut not exactly parallel to its long axis. A round cell (bright yellow) surrounded by a collagen-free region at the lower end suggested growth in that direction which happened to be pointing towards the first artery Figure S8 [C].
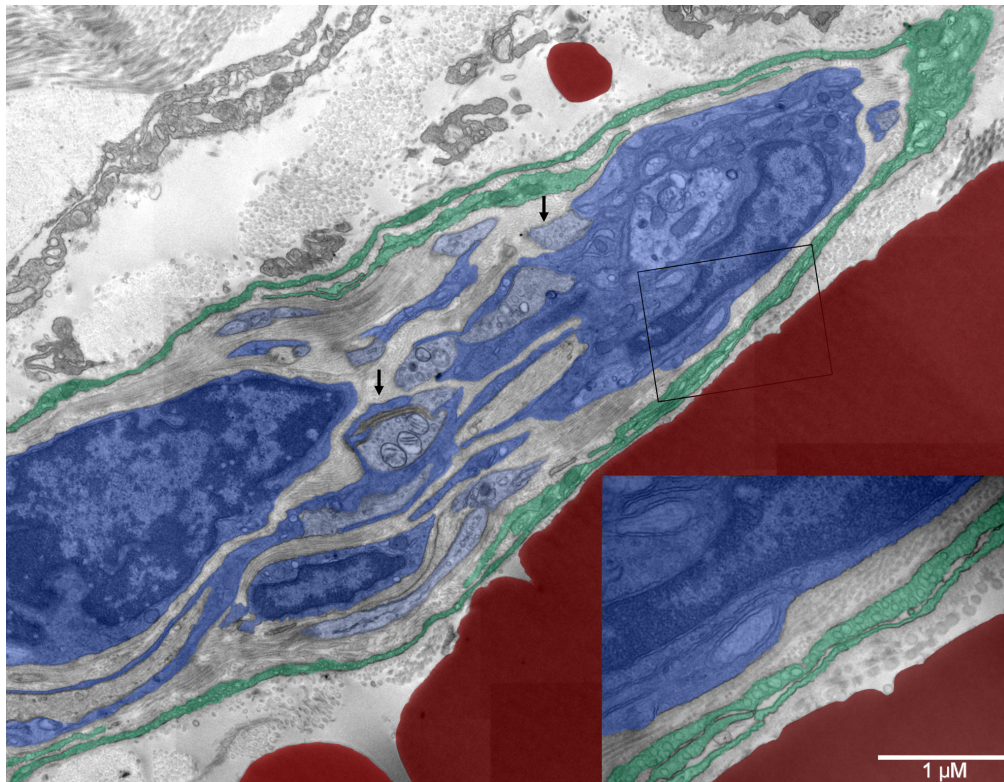
Figure S14. Developing peripheral nerve. Several nerve fibers (light blue) were engulfed by Schwann cells (dark blue) on the right but progressing myelination could be recognized only on the one in the center with three mitochondria in the section plane (left arrow). Multiple nerve boutons with synaptic vesicles (right arrow) were present but mature synapses were absent. Surrounding the nerve fibers was one to three-layer neurothelium (emerald green) with abundant caveolae (insert in the right lower corner). Collagen fibers located internally were thinner (20–40 nm) than those lining the external surface of the neurothelium (60–100 nm). A giant erythroschizosome (red) was located next to the forming nerve and it had similar dimensions (right lower corner behind the insert).
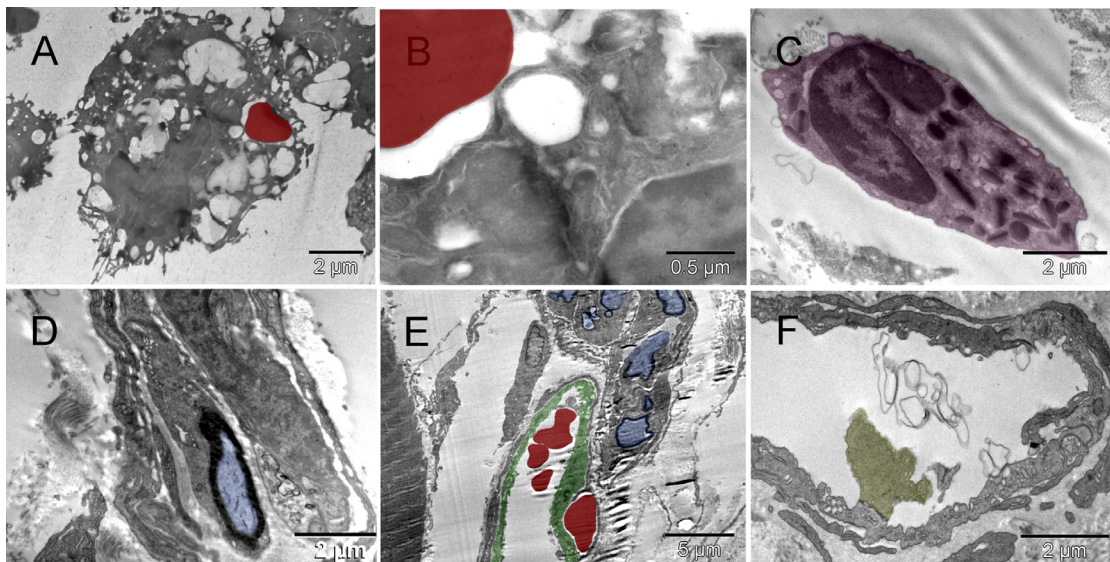
Figure S15. Rare findings. [**A** & **B**] Erythrosome labeled with ubiquitin-detecting antibody, internalized by non-labeled macrophage (Mouse 5). [**C**] Eosinophil (Mouse 3). [**D**]: Myelinated nerve fiber (blue) engulfed by Schwann cell (Mouse 2). [**E**] Forming vessel (green) located between muscle and nerves (Mouse 2). [**F**] Empty vein or lymphatic vessel with an internal valve (olive green) (Mouse 2).

References

1. Vidal M, Cusick ME, Barabasi AL: **Interactome networks and human disease.** *Cell.* 2011; **144**(6): 986–998.
   PubMed Abstract | **Publisher Full Text** | **Free Full Text**

2. Nurse P: **The great ideas of biology.** *Clin Med.* 2003; **3**(6): 560–568.
   **PubMed Abstract** | **Publisher Full Text**

3. Yoder MC, Ingram DA: **Endothelial progenitor cell: ongoing controversy for defining these cells and their role in neoangiogenesis in the murine system.** *Curr Opin Hematol.* 2009; **16**(4): 269–273.
   PubMed Abstract | **Publisher Full Text**

4. Zeigler BM, Sugiyama D, Chen M, *et al.*: **The allantois and chorion, when isolated before circulation or chorio-allantoic fusion, have hematopoietic potential.** *Development.* 2006; **133**(21): 4183–4192.
   PubMed Abstract | **Publisher Full Text**

5. Ueno H, Weissman IL: **The origin and fate of yolk sac hematopoiesis: application of chimera analyses to developmental studies.** *Int J Dev Biol.* 2010; **54**(6–7): 1019–1031.
   PubMed Abstract | **Publisher Full Text**

6. Gadue P, Weiss MJ: **Stem cells unscramble yolk sac hematopoiesis.** *Blood.* 2009; **114**(8): 1455–1456.
   PubMed Abstract | **Publisher Full Text**

7. Klimchenko O, Mori M, Distefano A, *et al.*: **A common bipotent progenitor generates the erythroid and megakaryocyte lineages in embryonic stem cell-derived primitive hematopoiesis.** *Blood.* 2009; **114**(8): 1506–1517.
   PubMed Abstract | **Publisher Full Text**

8. Geissmann F, Manz MG, Jung S, *et al.*: **Development of monocytes, macrophages, and dendritic cells.** *Science.* 2010; **327**(5966): 656–661.
   PubMed Abstract | **Publisher Full Text** | **Free Full Text**

9. Hanahan D, Weinberg RA: **Hallmarks of cancer: the next generation.** *Cell.* 2011; **144**(5): 646–674.
   PubMed Abstract | **Publisher Full Text**

10. Folkman J: **Anti-angiogenesis: new concept for therapy of solid tumors.** *Ann Surg.* 1972; **175**(3): 409–416.
    PubMed Abstract | **Publisher Full Text** | **Free Full Text**

11. Asahara T, Murohara T, Sullivan A, *et al.*: **Isolation of putative progenitor endothelial cells for angiogenesis.** *Science.* 1997; **275**(5302): 964–967.
    PubMed Abstract | **Publisher Full Text**

12. Purhonen S, Palm J, Rossi D, *et al.*: **Bone marrow-derived circulating endothelial precursors do not contribute to vascular endothelium and are not needed for tumor growth.** *Proc Natl Acad Sci U S A.* 2008; **105**(18): 6620–6625.
    PubMed Abstract | **Publisher Full Text** | **Free Full Text**

13. McGrath K, Palis J: **Ontogeny of erythropoiesis in the mammalian embryo.** *Curr Top Dev Biol.* 2008; **82**: 1–22.
    PubMed Abstract | **Publisher Full Text**

14. Sangiorgi F, Woods CM, Lazarides E: **Vimentin downregulation is an inherent feature of murine erythropoiesis and occurs independently of lineage.** *Development.* 1990; **110**(1): 85–96.
    PubMed Abstract

15. Palis J, Robertson S, Kennedy M, *et al.*: **Development of erythroid and myeloid progenitors in the yolk sac and embryo proper of the mouse.** *Development.* 1999; **126**(22): 5073–5084.
    PubMed Abstract

16. Palis J, Malik J, McGrath KE, *et al.*: **Primitive erythropoiesis in the mammalian embryo.** *Int J Dev Biol.* 2010; **54**(6–7): 1011–1018.
    PubMed Abstract | **Publisher Full Text**

17. Dzierzak E, Speck NA: **Of lineage and legacy: the development of mammalian hematopoietic stem cells.** *Nat Immunol.* 2008; **9**(2): 129–136.
    PubMed Abstract | **Publisher Full Text** | **Free Full Text**

18. Yoder MC, Hiatt K, Dutt P, *et al.*: **Characterization of definitive lymphohematopoietic stem cells in the day 9 murine yolk sac.** *Immunity.* 1997; **7**(3): 335–344.
    PubMed Abstract | **Publisher Full Text**

19. Schlitt HJ, Schafers S, Deiwick A, *et al.*: **Extramedullary erythropoiesis in human liver grafts.** *Hepatology.* 1995; **21**(3): 689–696.
    PubMed Abstract | **Publisher Full Text**

20. Costa-Val R, Nunes TA, Silva RC, *et al.*: **Inhibition of rats extramedullary liver erytropoiesis by hyperbaric oxygen therapy.** *Acta Cir Bras.* 2007; **22**(2): 137–141.
    PubMed Abstract | **Publisher Full Text**

21. Han J, Koh YJ, Moon HR, *et al.*: **Adipose tissue is an extramedullary reservoir for functional hematopoietic stem and progenitor cells.** *Blood.* 2010; **115**(5): 957–964.
    PubMed Abstract | **Publisher Full Text**

22. Maliszewski M, Majchrzak H, Ladzinski P, *et al.*: **[Extramedullary erythropoiesis in cerebellar hemangioblastomas].** *Neurol Neurochir Pol.* 1995; **29**(5): 713–722.
    PubMed Abstract

23. Mathews MS, Duma CM, Brant-Zawadzki M, *et al.*: **Extramedullary hematopoeisis within a convexity meningioma.** *Surg Neurol.* 2008; **69**(5): 522–525.
    PubMed Abstract | **Publisher Full Text**

24. Kuhn E, Dorji T, Rodriguez J, *et al.*: **Extramedullary erythropoiesis in chronic subdural hematoma simulating metastatic small round cell tumor.** *Int J Surg Pathol.* 2007; **15**(3): 288–291.

25. Skutelsky E, Danon D: **An electron microscopic study of nuclear elimination from the late erythroblast.** *J Cell Biol.* 1967; **33**(3): 625–635.
    PubMed Abstract | **Publisher Full Text** | **Free Full Text**

26. Simpson CF, Kling JM: **The mechanism of denucleation in circulating erythroblasts.** *J Cell Biol.* 1967; **35**(1): 237–245.
    PubMed Abstract | **Publisher Full Text** | **Free Full Text**

27. Rajapakse I, Perlman MD, Scalzo D, *et al.*: **The emergence of lineage-specific chromosomal topologies from coordinate gene regulation.** *Proc Natl Acad Sci U S A.* 2009; **106**(16): 6679–6684.
    PubMed Abstract | **Publisher Full Text** | **Free Full Text**

28. Gold P, Freedman SO: **Specific carcinoembryonic antigens of the human digestive system.** *J Exp Med.* 1965; **122**(3): 467–481.
    PubMed Abstract | **Publisher Full Text** | **Free Full Text**

29. Weinhouse S: **Glycolysis, respiration, and anomalous gene expression in experimental hepatomas: G.H.A. Clowes memorial lecture.** *Cancer Res.* 1972; **32**(10): 2007–2016.
    PubMed Abstract

30. Abelev GI: **Alpha-fetoprotein as a marker of embryo-specific differentiations in normal and tumor tissues.** *Transplant Rev.* 1974; **20**: 3–37.
    PubMed Abstract

31. Hammarström S: **The carcinoembryonic antige, and (CEA) family: structures, suggested functions and expression in normal and malignant tissues.** *Semin Cancer Biol.* 1999; **9**(2): 67–81.
    PubMed Abstract | **Publisher Full Text**

32. Sood AK, Fletcher MS, Hendrix MJ: **The embryonic-like properties of aggressive human tumor cells.** *J Soc Gynecol Investig.* 2002; **9**(1): 2–9.
    PubMed Abstract

33. McDonald DM, Munn L, Jain RK: **Vasculogenic mimicry: how convincing, how novel, and how significant?** *Am J Pathol.* 2000; **156**(2): 383–388.
    PubMed Abstract | **Publisher Full Text** | **Free Full Text**

34. Li L, Connelly MC, Wetmore C, *et al.*: **Mouse embryos cloned from brain tumors.** *Cancer Res.* 2003; **63**(11): 2733–2736.
    PubMed Abstract

35. Pierce GB, Aguilar D, Hood G, *et al.*: **Trophectoderm in control of murine embryonal carcinoma.** *Cancer Res.* 1984; **44**(9): 3987–3996.
    PubMed Abstract

36. Potten CS, Loeffler M: **Stem cells: attributes, cycles, spirals, pitfalls and uncertainties. Lessons for and from the crypt.** *Development.* 1990; **110**(4): 1001–1020.
    PubMed Abstract

37. Loeffler M, Roeder I: **Tissue stem cells: definition, plasticity, heterogeneity, self-organization and models–a conceptual approach.** *Cells Tissues Organs.* 2002; **171**(1): 8–26.
    PubMed Abstract | **Publisher Full Text**

38. Roeder I, Loeffler M: **A novel dynamic model of hematopoietic stem cell organization based on the concept of within-tissue plasticity.** *Exp Hematol.* 2002; **30**(8): 853–861.
    PubMed Abstract | **Publisher Full Text**

39. Loeffler M, Roeder I: **Conceptual models to understand tissue stem cell organization.** *Curr Opin Hematol.* 2004; **11**(2): 81–87.
    PubMed Abstract

40. Lander AD: **The 'stem cell' concept: is it holding us back?** *J Biol.* 2009; **8**(8): 70.
    PubMed Abstract | **Publisher Full Text** | **Free Full Text**

41. Salipante SJ, Kas A, McMonagle E, *et al.*: **Phylogenetic analysis of developmental and postnatal mouse cell lineages.** *Evol Dev.* 2010; **12**(1): 84–94.
    PubMed Abstract | **Publisher Full Text** | **Free Full Text**

42. Glauche I, Moore K, Thielecke L, *et al.*: **Stem cell proliferation and quiescence–two sides of the same coin.** *PLoS Comput Biol.* 2009; **5**(7): e1000447.
    PubMed Abstract | **Publisher Full Text** | **Free Full Text**

43. Witkiewicz H, Oh P, Schnitzer JE: **II. Capsular vaso-mimicry formed by transgenic mammary tumor spheroids implanted ectopically into mouse dorsal skin fold - cellular mechanisms of metastasis [v1; ref status: awaiting peer review, http://f1000r.es/9z].** *F1000 Res.* 2013; **2**(9).
    Publisher Full Text | **Free Full Text**

44. Torres Filho IP, Hartley-Asp B, Borgström P: **Quantitative angiogenesis in a syngeneic tumor spheroid model.** *Microvasc Res.* 1995; **49**(2): 212–226.
    PubMed Abstract | **Publisher Full Text**

45. Frost GI, Borgström P: **Real time *in vivo* quantitation of tumor angiogenesis.** *Methods Mol Med.* 2003; **85**: 65–78.
    PubMed Abstract | **Publisher Full Text**

46. Som PM, Brandwein M, Silvers AR, *et al.*: **Sialoblastoma (embryoma): MR findings of a rare pediatric salivary gland tumor.** *AJNR Am J Neuroradiol.* 1997; **18**(5): 847–850.
    PubMed Abstract

47. Liao MJ, Zhang CC, Zhou B, *et al.*: **Enrichment of a population of mammary**

gland cells that form mammospheres and have *in vivo* repopulating activity. *Cancer Res.* 2007; **67**(17): 8131–8138.
PubMed Abstract | **Publisher Full Text**

48. Nanni P, Pupa SM, Nicoletti G, *et al.*: **p185(neu) protein is required for tumor and anchorage-independent growth, not for cell proliferation of transgenic mammary carcinoma.** *Int J Cancer.* 2000; **87**(2): 186–194.
PubMed Abstract | **Publisher Full Text**

49. Cuadros C, Dominguez AL, Frost GI, *et al.*: **Cooperative effect between immunotherapy and antiangiogenic therapy leads to effective tumor rejection in tolerant Her-2/neu mice.** *Cancer Res.* 2003; **63**(18): 5895–5901.
PubMed Abstract

50. Oh P, Borgström P, Witkiewicz H, *et al.*: **Live dynamic imaging of caveolae pumping targeted antibody rapidly and specifically across endothelium in the lung.** *Nat Biotechnol.* 2007; **25**(3): 327–337.
PubMed Abstract | **Publisher Full Text** | **Free Full Text**

51. Hanaichi T, Sato T, Iwamoto T, *et al.*: **A stable lead by modification of Sato's method.** *J Electron Microsc (Tokyo).* 1986; **35**(3): 304–306.
PubMed Abstract

52. Tokuyasu KT: **Application of cryoultramicrotomy to immunocytochemistry.** *J Microsc.* 1986; **143**(Pt 2): 139–149.
PubMed Abstract | **Publisher Full Text**

53. Tober J, Koniski A, McGrath KE, *et al.*: **The megakaryocyte lineage originates from hemangioblast precursors and is an integral component both of primitive and of definitive hematopoiesis.** *Blood.* 2007; **109**(4): 1433–1441.
PubMed Abstract | **Publisher Full Text** | **Free Full Text**

54. Rieger MA, Smejkal BM, Schroeder T: **Improved prospective identification of megakaryocyte-erythrocyte progenitor cells.** *Br J Haematol.* 2009; **144**(3): 448–451.
PubMed Abstract | **Publisher Full Text**

55. Kim M, Cooper DD, Hayes SF, *et al.*: **Rhodamine-123 staining in hematopoietic stem cells of young mice indicates mitochondrial activation rather than dye efflux.** *Blood.* 1998; **91**(11): 4106–4117.
PubMed Abstract

56. Parise LV, Smyth SS, Coller BS: **Platelet morphology biochemistry and function. Chapter 111 in Williams Hematology**. 2001; 1357–1408 (ISBN 0-07-116293-3).
Reference Source

57. Ford Bainton D: **Morphology of neutrophils, eosinophils, and basophils. Chapter 64 in Williams Hematology**. 2001; 729–743 (ISBN 0-07-116293-3).
Reference Source

58. Subasinghe W, Spence DM: **Simultaneous determination of cell aging and ATP release from erythrocytes and its implications in type 2 diabetes.** *Anal Chim Acta.* 2008; **618**(2): 227–233.
PubMed Abstract | **Publisher Full Text** | **Free Full Text**

59. Dvorak AM, Kohn S, Morgan ES, *et al.*: **The vesiculo-vacuolar organelle (VVO): a distinct endothelial cell structure that provides a transcellular pathway for macromolecular extravasation.** *J Leukoc Biol.* 1996; **59**(1): 100–115.
PubMed Abstract

60. Idé C, Saito T: **Adenosine triphosphatase activity of cutaneous nerve fibers.** *Histochemistry.* 1980; **65**(2): 83–92.
PubMed Abstract | **Publisher Full Text**

61. Nasu F, Inomata K: **Ultracytochemical demonstration of Ca2(+)-ATPase activity in the rat saphenous artery and its innervated nerve terminal.** *J Electron Microsc (Tokyo).* 1990; **39**(6): 487–491.
PubMed Abstract

62. Fujimoto T: **Calcium pump of the plasma membrane is localized in caveolae.** *J Cell Biol.* 1993; **120**(5): 1147–1157.
PubMed Abstract | **Publisher Full Text** | **Free Full Text**

63. Schnitzer JE, Oh P, Jacobson BS, *et al.*: **Caveolae from luminal plasmalemma of rat lung endothelium: microdomains enriched in caveolin, Ca(2+)-ATPase, and inositol trisphosphate receptor.** *Proc Natl Acad Sci U S A.* 1995; **92**(5): 1759–1763.
PubMed Abstract | **Publisher Full Text** | **Free Full Text**

64. Brown JM, Giaccia AJ: **The unique physiology of solid tumors: opportunities (and problems) for cancer therapy.** *Cancer Res.* 1998; **58**(7): 1408–1416.
PubMed Abstract

65. Bertossi M, Roncali L, Nico B, *et al.*: **Ultrastructure and permeability of immature neural and extraneural blood vessels.** *Biol Struct Morphog.* 1990; **3**(1): 37–44.
PubMed Abstract

66. Wolff JR, Goerz C, Bär T, *et al.*: **Common morphogenetic aspects of various organotypic microvascular patterns.** *Microvasc Res.* 1975; **10**(3): 373–395.
PubMed Abstract | **Publisher Full Text**

67. Gurdon JB: **The developmental capacity of nuclei taken from intestinal epithelium cells of feeding tadpoles.** *J Embryol Exp Morphol.* 1962; **10**: 622–640.
PubMed Abstract

68. Takahashi K, Yamanaka S: **Induction of pluripotent stem cells from mouse embryonic and adult fibroblast cultures by defined factors.** *Cell.* 2006; **126**(4): 663–676.
PubMed Abstract | **Publisher Full Text**

69. Krawczyk A, Izdebska M, Grzanka A: **[The influence of hyperglycemia on functions of endothelial progenitor cells].** *Pol Merkur Lekarski.* 2009; **26**(153): 245–247.
PubMed Abstract

70. Blau HM, Baltimore D: **Differentiation requires continuous regulation.** *J Cell Biol.* 1991; **112**(5): 781–783.
PubMed Abstract | **Publisher Full Text** | **Free Full Text**

71. Tsang AP, Fujiwara Y, Hom DB, *et al.*: **Failure of megakaryopoiesis and arrested erythropoiesis in mice lacking the GATA-1 transcriptional cofactor FOG.** *Genes Dev.* 1998; **12**(8): 1176–1188.
PubMed Abstract | **Free Full Text**

72. Randrianarison-Huetz V, Laurent B, Bardet V, *et al.*: **Gfi-1B controls human erythroid and megakaryocytic differentiation by regulating TGF-beta signaling at the bipotent erythro-megakaryocytic progenitor stage.** *Blood.* 2010; **115**(14): 2784–2795.
PubMed Abstract | **Publisher Full Text**

73. Ribatti D: **Hemangioblast does exist.** *Leuk Res.* 2008; **32**(6): 850–854.
PubMed Abstract | **Publisher Full Text**

74. Soda Y, Marumoto T, Friedmann-Morvinski D, *et al.*: **Transdifferentiation of glioblastoma cells into vascular endothelial cells.** *Proc Natl Acad Sci U S A.* 2011; **108**(11): 4274–4280.
PubMed Abstract | **Publisher Full Text** | **Free Full Text**

75. Nishikawa SI, Nishikawa S, Kawamoto H, *et al.*: **In vitro generation of lymphohematopoietic cells from endothelial cells purified from murine embryos.** *Immunity.* 1998; **8**(6): 761–769.
PubMed Abstract | **Publisher Full Text**

76. Robin C, Durand C: **The roles of BMP and IL-3 signaling pathways in the control of hematopoietic stem cells in the mouse embryo.** *Int J Dev Biol.* 2010; **54**(6–7): 1189–1200.
PubMed Abstract | **Publisher Full Text**

77. Kitchen SM, Kempston T, Alberts AS: **Endometrial Hyperplasia Resulting from Myeloid-Specific Targeting of the Tumor Suppressor APC: Epithelium Arising from Bone Marrow Progenitors?** 2009; 5–5.

78. Zovein AC, Hofmann JJ, Lynch M, *et al.*: **Fate tracing reveals the endothelial origin of hematopoietic stem cells.** *Cell Stem Cell.* 2008; **3**(6): 625–636.
PubMed Abstract | **Publisher Full Text** | **Free Full Text**

79. Lach B, Gregor A, Rippstein P, *et al.*: **Angiogenic histogenesis of stromal cells in hemangioblastoma: ultrastructural and immunohistochemical study.** *Ultrastruct Pathol.* 1999; **23**(5): 299–310.
PubMed Abstract

80. Bjornson CR, Rietze RL, Reynolds BA, *et al.*: **Turning brain into blood: a hematopoietic fate adopted by adult neural stem cells *in vivo*.** *Science.* 1999; **283**(5401): 534–537.
PubMed Abstract

81. Jackson KA, Mi T, Goodell MA: **Hematopoietic potential of stem cells isolated from murine skeletal muscle.** *Proc Natl Acad Sci U S A.* 1999; **96**(25): 14482–14486.
PubMed Abstract | **Publisher Full Text** | **Free Full Text**

82. Gussoni E, Soneoka Y, Strickland CD, *et al.*: **Dystrophin expression in the mdx mouse restored by stem cell transplantation.** *Nature.* 1999; **401**(6751): 390–394.
PubMed Abstract | **Publisher Full Text**

83. Badorff C, Brandes RP, Popp R, *et al.*: **Transdifferentiation of blood-derived human adult endothelial progenitor cells into functionally active cardiomyocytes.** *Circulation.* 2003; **107**(7): 1024–1032.
PubMed Abstract | **Publisher Full Text**

84. Minana MD, Carbonell-Uberos F, Mirabet V, *et al.*: **IFATS collection: Identification of hemangioblasts in the adult human adipose tissue.** *Stem Cells.* 2008; **26**(10): 2696–2704.
PubMed Abstract | **Publisher Full Text**

85. Wurmser AE, Nakashima K, Summers RG, *et al.*: **Cell fusion-independent differentiation of neural stem cells to the endothelial lineage.** *Nature.* 2004; **430**(6997): 350–356.
PubMed Abstract | **Publisher Full Text**

86. Ogawa M, Larue AC, Watson PM, *et al.*: **Hematopoietic stem cell origin of connective tissues.** *Exp Hematol.* 2010; **38**(7): 540–547.
PubMed Abstract | **Publisher Full Text**

87. Witkiewicz H, Oh P, Schnitzer JE: **III. Cellular ultrastructures *in situ* as key to understanding tumor energy metabolism - biological significance of the Warburg effect [v1; ref status: awaiting peer review, http://f1000r.es/a0].** *F1000 Res.* 2013; **2**(10).
Publisher Full Text

88. Namazi MR, Fallahzadeh MK, Schwartz RA: **Strategies for prevention of scars: what can we learn from fetal skin?** *Int J Dermatol.* 2011; **50**(1): 85–93.
PubMed Abstract | **Publisher Full Text**

89. Wu DC, Paulson RF: **Hypoxia regulates BMP4 expression in the murine spleen during the recovery from acute anemia.** *PLoS One.* 2010; **5**(6): e11303.
PubMed Abstract | **Publisher Full Text** | **Free Full Text**

90. Goldman O, Feraud O, Boyer-Di Ponio J, *et al.*: **A boost of BMP4 accelerates the commitment of human embryonic stem cells to the endothelial lineage.** *Stem Cells.* 2009; **27**(8): 1750–1759.
PubMed Abstract | **Publisher Full Text**

91. Pearson S, Sroczynska P, Lacaud G, *et al.*: **The stepwise specification of embryonic stem cells to hematopoietic fate is driven by sequential exposure to Bmp4, activin A, bFGF and VEGF.** *Development.* 2008; **135**(8): 1525–1535.
PubMed Abstract | **Publisher Full Text**

92. Nardelli J, Thiesson D, Fujiwara Y, *et al.*: **Expression and genetic interaction of transcription factors GATA-2 and GATA-3 during development of the mouse**

central nervous system. *Dev Biol.* 1999; **210**(2): 305–321.
PubMed Abstract | **Publisher Full Text**

93. Olive PL, Vikse C, Trotter MJ: **Measurement of oxygen diffusion distance in tumor cubes using a fluorescent hypoxia probe.** *Int J Radiat Oncol Biol Phys.* 1992; **22**(3): 397–402.
PubMed Abstract | **Publisher Full Text**

94. Si ZC, Liu J: **What "helps" tumors evade vascular targeting treatment?** *Chin Med J (Engl).* 2008; **121**(9): 844–849.
PubMed Abstract

95. Eichmann A, Makinen T, Alitalo K: **Neural guidance molecules regulate vascular remodeling and vessel navigation.** *Genes Dev.* 2005; **19**(9): 1013–1021.
PubMed Abstract | **Publisher Full Text**

96. El Hallani S, Boisselier B, Peglion F, *et al.*: **A new alternative mechanism in glioblastoma vascularization: tubular vasculogenic mimicry.** *Brain.* 2010; **133**(Pt 4): 973–982.
PubMed Abstract | **Publisher Full Text**

97. Palmer TD, Willhoite AR, Gage FH: **Vascular niche for adult hippocampal neurogenesis.** *J Comp Neurol.* 2000; **425**(4): 479–494.
PubMed Abstract | **Publisher Full Text**

98. Mirzadeh Z, Merkle FT, Soriano-Navarro M, *et al.*: **Neural stem cells confer unique pinwheel architecture to the ventricular surface in neurogenic regions of the adult brain.** *Cell Stem Cell.* 2008; **3**(3): 265–278.
PubMed Abstract | **Publisher Full Text** | **Free Full Text**

99. Tavazoie M, van der V, Silva-Vargas V, *et al.*: **A specialized vascular niche for adult neural stem cells.** *Cell Stem Cell.* 2008; **3**(3): 279–288.
PubMed Abstract | **Publisher Full Text**

100. Shen Q, Wang Y, Kokovay E, *et al.*: **Adult SVZ stem cells lie in a vascular niche: a quantitative analysis of niche cell-cell interactions.** *Cell Stem Cell.* 2008; **3**(3): 289–300.
PubMed Abstract | **Publisher Full Text** | **Free Full Text**

101. Yang XT, Bi YY, Feng DF: **From the vascular microenvironment to neurogenesis.** *Brain Res Bull.* 2011; **84**(1): 1–7.
PubMed Abstract | **Publisher Full Text**

102. Alby L, Auerbach R: **Differential adhesion of tumor cells to capillary endothelial cells *in vitro*.** *Proc Natl Acad Sci U S A.* 1984; **81**(18): 5739–5743.
PubMed Abstract | **Publisher Full Text** | **Free Full Text**

103. Auerbach R, Alby L, Morrissey LW, *et al.*: **Expression of organ-specific antigens on capillary endothelial cells.** *Microvasc Res.* 1985; **29**(3): 401–411.
PubMed Abstract | **Publisher Full Text**

104. Auerbach R, Lu WC, Pardon E, *et al.*: **Specificity of adhesion between murine tumor cells and capillary endothelium: an *in vitro* correlate of preferential metastasis *in vivo*.** *Cancer Res.* 1987; **47**(6): 1492–1496.
PubMed Abstract

105. Pasqualini R, Ruoslahti E: **Organ targeting *in vivo* using phage display peptide libraries.** *Nature.* 1996; **380**(6572): 364–366.
PubMed Abstract | **Publisher Full Text**

106. St Croix B, Rago C, Velculescu V, *et al.*: **Genes expressed in human tumor endothelium.** *Science.* 2000; **289**(5482): 1197–1202.
PubMed Abstract | **Publisher Full Text**

107. Ruoslahti E, Rajotte D: **An address system in the vasculature of normal tissues and tumors.** *Annu Rev Immunol.* 2000; **18**: 813–827.
PubMed Abstract | **Publisher Full Text**

108. Reese TS, Karnovsky MJ: **Fine structural localization of a blood-brain barrier to exogenous peroxidase.** *J Cell Biol.* 1967; **34**(1): 207–217.
PubMed Abstract | **Publisher Full Text** | **Free Full Text**

Current Referee Status: ✗ ✓ ✓

- -

Referee Responses for Version 2

✓ **Karolina Kucharova**
Sanford-Burnham Medical Research Institute, La Jolla, CA, USA

Approved: 28 January 2014

Referee Report: 28 January 2014

I have read this submission. I believe that I have an appropriate level of expertise to confirm that it is of an acceptable scientific standard.

Competing Interests: No competing interests were disclosed.

✓ **Anita Bandrowski**
Division of Biological Sciences, University of California, San Diego, La Jolla, CA, USA

Approved: 22 July 2013

Referee Report: 22 July 2013
The authors addressed the main point of my criticism adequately. The number of animals in the report is now more clearly defined in table 1 and they are adequate to support the conclusions.

The other minor points seem to have been addressed throughout the manuscript.

I have read this submission. I believe that I have an appropriate level of expertise to confirm that it is of an acceptable scientific standard.

Competing Interests: No competing interests were disclosed.

✗ **Louise Purton**
Stem Cell Regulation Unit, St Vincent's Institute, Fitzroy, VIC, Australia

Not Approved: 15 July 2013

Referee Report: 15 July 2013
The authors have not sufficiently addressed my concerns in their response to my original assessment. My concerns remain the same.

I have read this submission. I believe that I have an appropriate level of expertise to state that I do not consider it to be of an acceptable scientific standard, for reasons outlined above.

Competing Interests: No competing interests were disclosed.

Referee Responses for Version 1

Karolina Kucharova
Sanford-Burnham Medical Research Institute, La Jolla, CA, USA

Approved: 30 May 2013

Referee Report: 30 May 2013

The title: "I. Embryonal vasculature formation recapitulated in transgenic mammary tumor spheroids implanted pseudo-orthotopicly into mouse dorsal skin fold: the organoblasts concept" is appropriate for the content of the article.

The abstract represents a suitable summary of the work.

The methods are well documented, except there is little information about the chamber that was implanted – that portion needs to be expanded (e.g. explain the chamber design, dimensions, material, the pore sizes). How the tumor spheroids were implanted into the chamber (e.g. injected by needle). Using the results section, I only assume that the chamber was made from glass and covered by a hyaline membrane.

The article is well constructed and is bringing a different opinion about angiogenesis in a tumor microenvironment. I appreciate that the authors moved their observation from *in vitro* to *in vivo* studies and emphasize the fact that the processes in the tumor microenvironment are very dynamic.

I appreciate that the authors studied cell morphology during their analyses rather than relying solely on immuno-markers.

If the authors prefer to use the original black and white microphotographs, then I suggest adding arrows, arrowheads and other symbols to the figures, figure legends, and text to indicate exactly which cells are being discussed – e.g. megakaryocytes or erythroblast in figure 1A. This type of correction should be carried on to all other figures.

Or the authors may switch the B/W Figure 1 with a color Figure S1 (there are the different cell types indicated by the colors).

In figure 5 and S5, I suggest adding arrows pointing at GFP positive structures.
In figure 10A and S10A, change the scale unit 'µM' to 'µm'.

The discussion seems longer than needed – I suggest that it should be cut to focus on the current results.

I have read this submission. I believe that I have an appropriate level of expertise to confirm that it is of an acceptable scientific standard.

Competing Interests: No competing interests were disclosed.

1 Comment

Author Response

Halina Witkiewicz, PRISM, USA
Posted: 03 Jul 2013

The scale bar unit in Figures 10 [A] & S10 [A] has been corrected. The details of setting up the chambers have been described in references 44, 45 & 50.
Competing Interests: No competing interests were disclosed.

Anita Bandrowski
Division of Biological Sciences, University of California, San Diego, La Jolla, CA, USA

Approved with reservations: 08 May 2013

Referee Report: 08 May 2013
The paper entitled 'I. Embryonal vasculature formation recapitulated in transgenic mammary tumour spheroids implanted pseudo-orthotopically into mouse dorsal skin fold: the organoblasts concept' by Witkiewicz, Oh and Schnitzer presents a novel and interesting view of vasculature development in solid tumours. The notion that tumour cells become organized into a pseudo organ, complete with its' own division of labour is compelling. The methods and results reported herein show a significant meticulous scholarship in this group. The work is of a high quality and the paper is generally well written.

The reporting of methods is refreshingly complete, but a few things should be clarified. In a recent announcement of Nature's policies on methods reporting (see http://www.nature.com/authors/policies/checklist.pdf) several items are pointed out as critical, which the authors address; they provide stock numbers for animals, catalogue numbers for significant reagents, the order of procedures and most of the other characteristics specified as significant. The parts of the methods that must be clarified are: The n's could be made explicit throughout the paper; and the reasons that incubation in addition to graft tissue differed between figures 1-8 vs 9+ should be clarified by the authors before final approval.

As the first reviewer correctly points out, the interpretation of ultra-structural data can be an art, and it is my opinion that the only way to get a good sense of these figures is to bring the community in, allowing them to see the full size images and manipulate them. There are projects that collect images that are full size and allow the community to view and manipulate the data sets, comparing images from different data sets and deploying automated tools to align them (the cell: an image library cellimagelibrary.org or the Cell Centered DataBase ccdb.ucsd.edu). While this step is not required, it may be a good way to increase the visibility of the data and allow multiple parties to weigh in on interpretation.

The conclusions presented in the study are coherent with the data, but at odds with a prevailing theory. The authors bring up the point that "the views on tumour neo-angiogenesis have remained polarized and we have yet to stop tumour growth" in no uncertain terms bringing ire from the community. The statement may not be completely fair, but given the lack of ability of independent researchers to reproduce most significant cancer studies (Nature 483, 531–533) it may not be unfounded and again it may generate controversy, spurring others to repeat the work presented here. If the work stands the test of time and the ire of the community, the implications will be profound.

A set of minor points are found below.

RT is not defined as acronym, seems to be room temperature, but should be stated
Perhaps a table of acronyms found in the paper would help in readability?

Please rewrite this sentence to clarify your point;

'The presence of a composite dense body, characteristic of platelets[56], in an extra-cellular matrix (ECM) producer indicated that the ECM building cell was related to megakaryocyte (Figure 1[E & F]).'

I have read this submission. I believe that I have an appropriate level of expertise to confirm that it is of an acceptable scientific standard, however I have significant reservations, as outlined above.

Competing Interests: No competing interests were disclosed.

1 Comment

Author Response

Halina Witkiewicz, PRISM, USA
Posted: 03 Jul 2013

This and the two accompanying articles report results of basic research on tumor biology. The rules regarding 'n's and controls required for pre-clinical pharmacological studies do not apply here because we did not test any treatment or hypothesis for a mechanism of action of a potential new drug. The article describes phenomena that *in vivo* occur simultaneously, side by side, because unlike in embryo, the tumors keep growing but never mature. Total 5 mice were used to make observations that were unprecedented and consistently corrected the erroneous belief lasting since 1967 regarding the mechanism of erythrocyte enucleation by nuclear expulsion (Skutelsky & Danon, *J Cell Biol* (1967); Simpson & Kling, *J Cell Biol* (1967)). In those two publications, the numbers of mice or dogs used for the ultrastructural analysis *in situ* were not mentioned. For our purposes, the numbers of animals with pseudo-orthotopicly and ectopicly implanted tumor spheroids (n=3 and n=2, respectively) appear adequate. A link to the image library will be provided when the images are deposited. Other critical comments made by the referee have been addressed in the amended version of the article.
Competing Interests: No competing interests were disclosed.

Louise Purton
Stem Cell Regulation Unit, St Vincent's Institute, Fitzroy, VIC, Australia

Not Approved: 14 January 2013

Referee Report: 14 January 2013

The authors rely heavily on their own identification of ultrastructure components of cells without any confirmation of the identity of the cells by immunostaining. Furthermore, all of the immunostaining they do show is questionable and likely non-specific staining (in the materials and methods the appropriate species-matched isotype control is not listed, the one that is listed is of incorrect species). While megakaryocytes and erythrocytes are easily morphologically identifiable, I disagree with their interpretation of the data at 5 days, when they state that no endothelial cells are visible. My opinion is that an EC is visible in Figure 1C at the bottom (they claim this is a megakaryocyte). The authors are strongly advised to read papers by Leon Weiss, who did excellent TEM studies of mouse bone marrow and is the expert in this field. Without confirmation of the different cell types in this study with specific immunostaining their conclusions are not valid. Larger numbers of mice at each time point are also required to show reproducibility of findings.

I have read this submission. I believe that I have an appropriate level of expertise to state that I do not consider it to be of an acceptable scientific standard, for reasons outlined above.

Competing Interests: No competing interests were disclosed.

1 Comment

Author Response

Halina Witkiewicz, PRISM, USA
Posted: 10 Apr 2013

Identifying cells
The referee's notion that we rely heavily on cellular morphology (at the ultrastructural level) is accurate. To that experimental approach we devoted the opening section of the Discussion in the accompanying article (III) because we believe it is the strength of our study.

The referee's generic skepticism with regard to usefulness of morphological features for identifying cell phenotypes is inconsistent with her other statements. On one hand she states that "Without confirmation of the different cell types … with specific immunostaining… conclusions are not valid" and on the other that "… megakaryocytes and erythrocytes are easily morphologically identifiable…" and goes on to identify a cell in Figure 2 as endothelial (EC) - without confirmation with the specific immunostaining. However, the cell in question does not fulfill the criteria that we used for the EC phenotype, namely: a flattened shape, polarized cell membrane with abundant caveolae (mostly on luminal surface) and attachment to collagen or basement membrane (on abluminal surface), collagen synthesis and occasionally seen Weibel-Palade bodies (page 10 of the accompanying article III).

Moreover, *in vivo* mature -thelial cells of any kind (endo-, epi- or meso-) have tight contacts with one another. That is how ECs can be identified also in absence of erythrosomes (in sections of tissues fixed by perfusion). In contrast, the hallmarks of megakaryocyte are: large nuclei often containing double nucleoli, large asymmetrically distributed irregularly shaped cytoplasm and satellite platelets (Figure 1 [A] and 2 [B]). The referee does not specify criteria by which the cell in Figure 2 was in her opinion an EC and not a megakaryocyte.

Antibodies

The referee questions specificity of the antibodies that we used: GFP-specific rabbit polyclonal IgG (ab290) from Abcam; calmyrin-specific rabbit polyclonal IgG (11823-1-AP) from ProteinTech Group, Inc. and CD34-specific monoclonal IgG$_{2a}$ (sc-18917) from Santa Cruz. All those vendors validated the specificity of the antibodies in ways presented in their datasheets. Abcam and Santa Cruz also provided references to published work by authors who used the antibodies successfully.

Nevertheless, each experimental setting requires controls addressing issues specific for that setting. Out of 150 publications that used the GFP-specific antibody only one had the species matched isotype control and out of 15 that used the CD34-specific antibody also only one had it. Both reported flow cytometry studies.

For *in situ* analysis the best controls are the internal ones, demonstrating variable pattern of staining that correlates with particular ultrastructures as expected based on the experimental design. We showed those. The pattern of GFP-specific immunostaining depended on the promoter controlling expression of the inserted GFP coding sequence. In case of the ubiquitin promoter the label was ubiquitous, including erythrosomes, whereas in case of the histone H2B promoter the label was associated with chromatin, regardless of the cell cycle phase (inter-phase nucleus or mitotic chromosomes), although not in all cells because neither the host nor the graft donor mouse contained the GFP. Therefore the erythrosome labeled with anti-ubiquitin antibody and internalized by unlabeled macrophage must have been of the graft origin (Figure 15 [A, B]). Similarly, the unlabeled fibroblast next to the labeled dividing tumor cell must have been of the host origin (Figure 2 [F] in the accompanying article II). Thus the same antibody produced different staining patterns in sections from differently handled host mice. Both were expected and easy to explain.

The variable distribution of calmyrin-associated Au grains correlated with the level of morphological complexity in the evolving phenotypes of HSC lineage (Figure 6 EFI & Figure 8). In emerging erythrosomes they were randomly dispersed initially and in more mature forms they appeared in distinct clusters, the calmyrites, whereas the CD34 label vanished from the nuclear area at the start of the nucleo-cytoplasmic conversion (Figure 4 [F]) and was not found in erythrosomes.

None of the three antibodies were essential in identifying particular phenotypes. CD34, thought of as a primitive stem cell marker, was present in various differentiated cells of HSC lineage as well, and the distinct clusters of Au particles attributed to calmyrites were present in even greater variety of differentiated cell types, including nonmalignant rat epithelium. Such clusters were not seen extracellularly. Finally, both the anti-GFP and anti-calmyrin antibodies were rabbit polyclonal IgGs and therefore, represented the species matched isotype controls for each other.

Numbers Our goal was accomplished by generating unprecedented photographic documentation of spontaneous inter-cellular relations leading to the vasculature formation. The animals were not subjected to any kind of treatment except implantation of the tumor. The nature of the study was exploratory and observational therefore the results were qualitative. The images represented raw data, i.e. a direct demonstration of the phenomena that had actually occurred *in vivo*. The conventional thinking in terms of comparing treated and control groups over a period of time to measure an anticipated effect and to evaluate its statistical significance was not applicable here. The time progression was not critical either, in contrast to the embryonal growth and development, because the tumor never matures.

In our model the cells were responding to locally variable microenvironment therefore they were

not functionally synchronized. Consequently a range of different stages of vasculature morphogenesis could be found simultaneously within single sections. To extend that range we did have two different times of incubating tumors in the skin fold chambers: one and three weeks. Indeed, different yet overlapping sets of options were found. However, in tumors grown for three weeks without the graft we found the earliest stages of vasculature morphogenesis (Figure 1) repeated in necrotic areas that were being repopulated. Thus the range of options was well covered.

To illustrate our conclusions we selected representative images after careful analysis of many (several hundreds per mouse at various magnifications). We stopped the analysis when the findings became redundant and we understood the observed phenomena. In the literature the number of studied animals tends to be inversely proportional to complexity of assays. For example, one study using ab290 involved animal groups of variable size: n = 18 for flow cytometry and n = 6 for histology (PM:15883207). For electron microscopy based studies it is common to use samples from small number of individuals (PM:20439620). In all five mice that we used (in this and the accompanying articles) the fundamental cellular mechanism of initiating the vasculature formation turned out to be the same. Thus, the number of animals was adequate for the goal of this particular study. Increasing the number of sacrificed animals above the necessary minimum, just for the number sake, would be superfluous and against the animal welfare rules.

Competing Interests: No competing interests were disclosed.